Recent Results from LEP

Joachim Mnich
CERN EP-L3
CH-1211 Genève 23

Abstract

This article summarises recent results obtained by the four experiments ALEPH, DELPHI, L3 and OPAL at the LEP e^+e^- collider. The experimental results discussed here comprise a summary of the measurements of electroweak observables at the Z resonance, the measurement of W-pair production from the threshold up to $\sqrt{s} = 189$ GeV and results from the searches for Higgs bosons and Supersymmetric particles at these highest energies attained in e^+e^- collisions.

Keywords: Z parameter, W mass, triple boson couplings, tests of electroweak interactions, Higgs bosons, Supersymmetry

1 Introduction

The Large Electron-Positron Collider (LEP) at CERN in Geneva started in 1989 to operate at centre-of-mass (cms) energies close to the mass of the Z boson. This first phase (LEP I) has been concluded in 1995. The four experiments collected a total of about 16 million decays of the Z into hadrons and leptons. This large data sample allows the very precise measurement of Z parameters and tests of the Standard Model [1] (SM) beyond the tree level. Many other physics results have been obtained, and are still obtained, from careful analyses of these data. Examples are tests of Quantum Chromodynamics (QCD) as well as physics of the b-quark and the tau lepton.

In the autumn of 1995 the LEP machine began to raise in steps the centre-of-mass energy beyond the Z resonance. This has been possible after installation of additional super-conducting radio frequency cavities required by the higher energy loss due to synchrotron radiation at higher beam energies. In preparation of the second phase (LEP II), marked by running at energies above the W pair production cross section, LEP was operated at cms energies between 130 and 140 GeV in November 1995. The W-pair production threshold of 161 GeV was reached in 1996 and the cms energy could be further increased to 172 GeV in the same year. The year after 183 GeV were attained and in

Year	$\sqrt{s}$	$\int\mathcal{L}\,\mathrm{d}t$
1995	130 – 140 GeV	5 pb^{-1}
1996	161/172 GeV	21 pb^{-1}
1997	183 GeV	55 pb^{-1}
	130/136 GeV	7 pb^{-1}
1998	189 GeV	180 pb^{-1}

Table 1: Summary of the LEP operation above the Z resonance. Listed are the approximate cms energies and the integrated luminosities collected on average by each experiment.

1998 a high luminosity run was performed at an energy of $\sqrt{s}$ = 189 GeV. Tab.1 summarises the cms energies and the approximate luminosities collected by each experiment.

At LEP II the experiments are performing measurements of the W-pair cross section $\mathrm{e^+e^-} \to \mathrm{W^+W^-}(\gamma)$ as function of the cms energy, the determination of the W mass and the study of triple gauge boson couplings. In addition, the increase in energy allows the exploration of new kinematic regions in the search for new particles, in particular for the SM Higgs boson [2] and Supersymmetric [3] (SUSY) particles. Other important fields investigated at LEP II are studies of fermion-pair production, tests of QCD and two-photon physics.

In this article selected items on these topics are presented: Precision tests of the SM at the Z resonance and above, W physics and the searches for Higgs bosons and SUSY particles. Most of the results presented here are preliminary, in particular those obtained at the highest energy reached in 1998, and they reflect the status of the analyses in spring 1999. All limits are at 95% confidence level (CL).

2 Physics of the Z Boson

One of the major achievements of the first phase of the LEP experiments is the precise measurement of cross sections around the Z resonance. Total cross section measurements are performed for the four reactions:

$$\begin{aligned} \mathrm{e^+e^-} &\to \mathrm{hadrons}(\gamma), & \mathrm{e^+e^-} &\to \mathrm{e^+e^-}(\gamma), \\ \mathrm{e^+e^-} &\to \mu^+\mu^-(\gamma), & \mathrm{e^+e^-} &\to \tau^+\tau^-(\gamma)\,. \end{aligned} \tag{1}$$

In the leptonic final states the forward-backward asymmetry is determined as well. As an example the total cross section $\mathrm{e^+e^-} \to \mathrm{hadrons}(\gamma)$ measured at the Z resonance is shown in Fig.1. The hadronic pole cross section is measured to an absolute precision of 0.1% by each of the four experiments. From these measurements the properties of the Z boson are derived with a precision which exceeds the expectations at the time the experiments began in 1989 [4].

As an example the combined results for the mass, total width and the partial hadronic and leptonic width of the Z are [5]:

$$\begin{aligned} m_{\rm Z} &= 91\,186.7 \pm 2.1 \text{ MeV}\,, & \Gamma_{\rm Z} &= 2\,493.9 \pm 2.4 \text{ MeV}\,, \\ \Gamma_{\rm had} &= 1\,742.3 \pm 2.3 \text{ MeV}\,, & \Gamma_{\ell} &= 83.90 \pm 0.10 \text{ MeV}\,. \end{aligned} \qquad (2)$$

In addition to the precise measurements of cross section an accurate knowledge of the LEP beam energy is mandatory to reach this experimental precision on Z parameters, in particular on the mass and the total width. The LEP energy could be calibrated to an accuracy of $\mathcal{O}(10^{-5})$ [6] which results in contributions to the errors on the mass and total width of approximately ± 1.7 MeV and ± 1.4 MeV, respectively. These uncertainties are included in the total errors given in Eq.2.

From the measured total and partial widths the partial decay width of the Z into invisible particles is derived to be $\Gamma_{\rm inv} = 500.1 \pm 1.9$ MeV which in turn yields for the number of neutrino families $N_\nu = 2.994 \pm 0.011$. This number is consistent with three which implies also that the couplings of the three known neutrino species to the Z are indeed as they are predicted in the SM. An upper limit on the Z decay width into other invisible particles is derived to be $\Gamma(\rm Z \to X_{inv}) < 2.8$ MeV which imposes constraints on models beyond the SM.

The measurements of forward-backward and left-right asymmetries as well as of tau-polarisation at the Z resonance allow the precise determination of the effective weak mixing angle $\sin^2\bar{\vartheta}_{\rm W}$. A comparison of $\sin^2\bar{\vartheta}_{\rm W}$ measurements is shown in Fig.2. Good agreement is observed between the results obtained from different observables and the average value is $\sin^2\bar{\vartheta}_{\rm W} = 0.23157 \pm 0.00018$ [5].

This measurement is compared to the SM calculation as a function of the Higgs mass using for the masses of the Z boson and the top quark and for the QED coupling constant α at $m_{\rm Z}$ the values indicated in the figure. The errors on these parameter lead to uncertainties in the calculation of $\sin^2\bar{\vartheta}_{\rm W}$ which are indicated by the bands. The measurements are consistent with Higgs masses between the lower bound given by the direct search for Higgs production at LEP (see Sec.6) and the upper theoretical limit of 1 TeV. The measured value of the weak mixing angle reveals a preference for a low value of $m_{\rm H}$. Together with other measurements this will be used in Sec.5 to derive the mass of the Higgs in the SM framework.

3 Fermion-Pair Production above the Z Resonance

The LEP experiments study fermion pair production at cms energies far above the Z resonance in the same channels as at the Z (Eq.1). However, at LEP II the total cross sections are about two orders of magnitude smaller.

At cms energies above the Z pole initial state radiation plays an important role. Radiation of one or more photons by the incoming electrons removes energy from the annihilation process and the fermion production takes place at a lower effective cms energy, $\sqrt{s'}$, where the cross section is different. In particular, if the remaining energy in the e^+e^- system is close to the mass of the Z the annihilation cross section is very high. Consequently this provides a major contribution to the total cross section $e^+e^- \to f\bar{f}$ and it is called radiative 'return-to-the-Z'. If the initial state photon is detected its measured energy can be used to calculate $\sqrt{s'}$. However, in general photons are emitted at small angles by the incoming electron or positron and thus often escape detection through the beam pipe. In this case the photon energy can be determined from the polar angles of the outgoing fermions.

The importance of the return-to-the-Z is illustrated in Fig.3 which shows the distribution of the effective cms energy for all LEP energies above the Z pole. Besides the peak at the nominal cms energy, with a smooth tail towards lower energies from the radiation of soft photons, one observes that a large fraction of the events is actually produced at $\sqrt{s'} \approx m_Z$.

Because of the different nature of events produced at, or close to, the nominal cms energy and those stemming from decays of real Z bosons the LEP experiments measure two sets of cross sections and forward-backward asymmetries: for the total sample and the high energy events separated by a cut in the reconstructed $\sqrt{s'}$ value. The definition of high energy events differs among the experiments.

The results of the total cross section measurements above the Z pole from the OPAL experiment are shown in Fig.4 for both the total event sample and the high energy events alone. The measurements are compared to the SM expectations as calculated with the programs ZFITTER [7] and, for $e^+e^- \to e^+e^-(\gamma)$, TOPAZ0 [8]. Good agreement is observed between the measurement and the SM prediction. Results and details on the analyses can be found in Ref. [9–12].

The measurements of total cross sections and forward-backward asymmetries are used to put constraints on new physics. A general framework for the description of new phenomena are four-fermion contact interactions [13]. Lower limits on the energy scale of such contact interactions, to be considered as the mass scale of exchanged virtual particles, are set by the LEP experiments in the order of 2 TeV $-$ 10 TeV, depending on the model and the final state. A summary is given in Fig.5. Other examples are lower mass limits on an additional neutral heavy boson, Z', which is ruled out up to a mass of 300 GeV. An hypothetical Z' boson with SM couplings to fermions must have a mass $m_{Z'} > 800$ GeV [14].

The hadronic events recorded during the runs at $130 \leq \sqrt{s} \leq 189$ GeV are used to perform studies on the energy evolution of observables and to compare them to the predictions based on QCD. For these studies events radiated to lower effective cms energies are excluded. Fig.6 compares the thrust distribution measured by the L3 experiment at $\sqrt{s} = 189$ GeV with various QCD based Monte Carlo models. Good agreement is observed and this thrust distribution, together with other event shape variables, is used to determine the strong

W $\to$	Measured [%]	SM [%]
hadrons	68.07 ± 0.42	67.5
eν	10.52 ± 0.26	
$\mu\nu$	10.56 ± 0.25	
$\tau\nu$	10.91 ± 0.34	
$\ell\nu$	10.64 ± 0.13	10.8

Table 2: Measured branching ratios of the W boson into hadrons, the three lepton families and the combined leptonic branching fraction.

coupling constant to be $\alpha_s(189\ \text{GeV}) = 0.1078 \pm 0.0028(\text{exp}) \pm 0.00523(\text{th})$ where the first error is experimental and the second reflects the theoretical uncertainty.

The large range of cms energies explored by the LEP experiments allows the measurement of the strong coupling constant α_s as function of energy. Running of α_s is clearly seen in Fig.7. The same event shape variables are used to determine α_s at the various energies such that the theoretical error is not affecting the measured energy dependence [15].

4 Physics of the W Boson

Since the threshold for W-pair production was attained in 1996 the LEP experiments study the reaction $e^+e^- \to W^+W^-(\gamma)$. The main goals are the measurement of the cross section as a function of the energy which, together with the measurement of differential cross sections, allows to study the couplings at the triple boson vertices, and the precise measurement of the W mass. Details on the analyses and published results on W physics at LEP can be found in Ref. [16–19].

Experimentally, three different topologies are distinguished in the production of W-pairs: purely leptonic $e^+e^- \to \ell\nu\ell\nu$ (ℓ = e, μ, τ), which contribute to about 11%, semi-leptonic $e^+e^- \to q\bar{q}\ell\nu$ (44%) and fully hadronic final states $e^+e^- \to q\bar{q}q\bar{q}$ (46%). Contributions to these final states from other processes, not involving two on-shell W bosons, have to be calculated from Monte Carlo simulation. Examples are single W production $e^+e^- \to We\nu$ and the exchange of two neutral bosons. Most difficult is the separation of the $e^+e^- \to q\bar{q}q\bar{q}$ signal from QCD four-jet events.

From the cross sections measured individually for the different final states the branching fractions of the W boson into hadrons and the three lepton species are derived (Tab.2) [20]. The decay rates into electrons, muons and taus are found to be equal and thus confirming lepton universality in charged current interactions. The measured hadronic decay width can be used to constrain the element V_{cs} of the Cabbibo-Kobayashi-Maskawa mixing matrix [21, 22] which is relatively badly known otherwise [23]. Assuming unitarity of the matrix one obtains $V_{\rm cs} = 1.002 \pm 0.016(\rm stat) \pm 0.012(\rm sys)$.

To date about 3500 $\rm e^+e^- \to W^+W^-(\gamma)$ events have been collected by each of the four collaborations, most of them at $\sqrt{s} = 183$ GeV and $\sqrt{s} = 189$ GeV. The average cross sections measured by the LEP experiments at cms energy values between the threshold and 189 GeV are shown in Fig.8 [20]. The measurements follow the SM expectation and prove the existence of triple gauge boson couplings. Hypotheses with no ZWW vertex or only t-channel exchange of electron neutrinos are ruled out.

More information on the couplings of the W boson is contained in the differential distributions of the W production angle and the decay angles in the W rest frame. Limits on anomalous couplings of the W boson to the photon and the Z are derived from combined fits to the observed distributions and the total cross sections.

Assuming the W couplings to be real, obeying C-, P- and CP- invariance and setting the electric charge of the W to be equal to that of the electron, the most general ansatz for W couplings reduces to five parameters. These parameters and their SM model values are:

$$g_1^{\rm Z} = 1\,, \qquad \kappa_\gamma = \kappa_{\rm Z} = 1\,, \qquad \lambda_\gamma = \lambda_{\rm Z} = 0\,. \tag{3}$$

The results for these coupling parameter obtained in likelihood fits leaving one parameter free at a time while fixing the others to their SM values are shown in Fig.9. Deviation from the SM values are denoted by Δ. All parameters are found to be consistent with their expected values and their experimental precision is at the 10% level. An example of a simultaneous determination for two parameters is shown in Fig.10.

Some of the above coupling parameters are constrained by low energy measurements as well as by the precision data from LEP I. Therefore, anomalous couplings are defined by linear combinations which do not alter the gauge boson propagators at tree level [24]:

$$\alpha_{{\rm W}\phi} = \Delta g_1^{\rm Z} \cos^2\vartheta_{\rm W}\,, \qquad \alpha_{\rm W} = \lambda_\gamma\,, \qquad \alpha_{{\rm B}\phi} = \Delta\kappa_\gamma - \Delta g_1^{\rm Z} \cos^2\vartheta_{\rm W}\,. \tag{4}$$

The results for this parametrisation are shown in Fig.11. In summary, the studies performed at LEP so far show no indication for anomalous W boson couplings.

An important measurement performed at LEP II is the precise determination of the mass of the W boson. A first value for $m_{\rm W}$ was derived from the total cross section measurement at the threshold, $\sqrt{s} = 161$ GeV, which is very sensitive to $m_{\rm W}$. The combined LEP result from this measurement is $m_{\rm W} = 80.40^{+0.22}_{-0.21}$ GeV.

At higher cms energies the W mass is obtained from direct reconstruction of the W decay products. To improve the resolution on the mass, a kinematic fit is performed using the precisely calibrated LEP beam energies. In addition, the masses of the two W bosons in an event are either constrained to be identical or the same within the width of the W.

Fig.12 shows the reconstructed W mass distributions obtained by OPAL from the 189 GeV data for the four different final states which can be used for this measurement. The data are compared to the result of the fit for m_{W}, indicating the contributions from the signal and the remaining background, the latter being important only in the four-jet and $\mathrm{q\bar{q}}\tau\nu$ channels. Published W mass measurement at LEP can be found in Ref. [25–28].

This method to measure the W mass can be checked on return-to-the-Z events. Here the Z mass is measured from its decay products applying the same method and detector calibrations used to determine m_{W}. Fig.13 shows the result of this exercise performed by L3 on the data sample taken at 183 GeV yielding a Z mass which is statistically compatible with the precise value obtained from the resonance curve (Eq.2).

A particular problem of the W mass measurement in $\mathrm{e^+e^-} \rightarrow \mathrm{q\bar{q}q\bar{q}}$ final states are interference effects between the decay products of the two different W bosons: Colour reconnection and Bose-Einstein correlations. The typical distance between the decay points of the two W bosons is 0.1 fm whereas the hadronisation scale of the quarks is a factor of ten larger. Hence, four naked, coloured quarks exist up to a distance of about 1 fm. Low energy gluons are exchanged between quarks from different W bosons implying a momentum transfer and hence a bias in the measurement of the invariant masses. Mesons consist the main part of hadronisation products of quarks. Obeying Bose-Einstein statistics they tend to occupy the same place in momentum space. As this holds also for mesons from different W bosons this again leads to a momentum transfer between them.

Both effects are difficult to model in Monte Carlo simulations. Estimates of the impact on the W mass measurement in the four-jet channel reach up to 100 MeV and consist an important source of systematic uncertainty. Using the data collected so far, and comparing the fragmentation of W bosons in $\mathrm{q\bar{q}q\bar{q}}$ and $\mathrm{q\bar{q}}\ell\nu$ events, extreme models can already be ruled out [29]. With the anticipated increase in statistics it should be possible to improve the modelling of the final state interference effects and to limit their impact on the W mass measurement.

The results for the W mass obtained at LEP from reconstruction of the decay products are [30] 80.313 ± 0.063 GeV for $\mathrm{q\bar{q}}\ell\nu$ and 80.429 ± 0.089 GeV for $\mathrm{q\bar{q}q\bar{q}}$ final states, the latter containing a contribution to the error from final state interference effects of 0.058 GeV. Combining all results obtained by the LEP experiments from the data taken above the WW threshold yields a value for the W mass of

$$m_{\mathrm{W}} = 80.350 \pm 0.056 \text{ GeV}\,. \tag{5}$$

The knowledge of the LEP energy is also important for this mass measurement and its absolute uncertainty contributes by ± 0.017 GeV to the error.

In addition, the total width of the W boson can be determined from the measured invariant mass distribution. As an example Fig.14 shows the result of a simultaneous fit to the W mass and width. The current results for the W width, including data up to $\sqrt{s} = 183$ GeV, are in in good agreement with the SM expectation and the precision is about 0.4 GeV per experiment.

5 Tests of the SM of Electroweak Interactions

The measurements discussed above of the properties of the heavy gauge bosons, the Z and $W^{\pm}$, are now used to test the SM of electroweak interactions at the tree level and beyond.

Firstly, measurements of the W mass obtained in very different ways are compared. Observables in $e^+e^- \to f\bar{f}$ at the Z resonance, in particular cross sections and asymmetries, determine the electroweak couplings. In the SM these couplings are related to the masses of the heavy gauge bosons, immediately evident from the on-shell definition of the weak mixing angle $\cos\vartheta_W = m_W/m_Z$. Results of measurements at the Z resonance can thus be converted into a mass of the W boson. It should be noted that m_W enters as parameter in lowest order formulae for observables. To derive the correct value from the measurements inclusion of higher order corrections is however mandatory.

On the other hand at LEP II, as well as at $p\bar{p}$ colliders, the mass of the W boson is directly measured from the invariant mass distribution of its decay products. Mass values from these two approaches are confronted in Fig.15. Their perfect agreement is an experimental confirmation of one of the cornerstones of the SM, namely the double role of the heavy gauge bosons as observable particles with masses determining electroweak couplings. Equivalently, the ratio of the W masses derived from the two approaches consist a measurement of the ρ-parameter which, apart from higher order corrections, is unity in the minimal SM with one Higgs doublet [31].

The experimental data available today allow tests of the SM beyond the tree level investigating higher corrections. Electroweak radiative corrections Δr arise, among others, from corrections to the gauge boson propagators. They relate the Fermi coupling constant G_F measured at very low momentum transfer from the muon lifetime to the heavy gauge boson masses [32]:

$$\frac{G_F}{\sqrt{2}} = \frac{\pi\alpha}{2} \frac{1}{m_W^2 \sin^2\vartheta_W} \frac{1}{1 - \Delta r} \tag{6}$$

One contribution to the electroweak radiative corrections is the running of the QED coupling constant α which introduces an uncertainty in SM calculations due to the contributions of hadronic loops [33]. Corrections to the $W^{\pm}$ and Z propagators arise from the large mass difference in the third quark doublet which is breaking the isospin symmetry and from Higgs boson loops. As a consequence, observables at the Z resonance depend, in first approximation, quadratically on the top quark mass and on the logarithm of the Higgs mass.

From precise measurements of electroweak observables the mass of the top quark can be inferred to be $m_t = 157^{+9}_{-8}$ GeV where the error includes our ignorance of the Higgs mass. This result is in good agreement with the direct measurement [23,34] $m_\mathrm{t} = 173.8 \pm 5.2$ GeV. Indeed, the mass of the top quark was rather precisely predicted before its discovery in 1994.

A comparison of direct and indirect mass determinations of the W and the top is shown in Fig.16. Agreement at the 68% CL level is observed for both masses and the conclusion is that the SM is correct at the 1-loop level. Also shown in Fig.16 is the SM prediction using the relation between G_F and m_W (Eq.6) for different Higgs masses ranging from the lower experimental bound (see Sec.6) to the upper theoretical limit. One notes that the measurements indicate a low mass for the Higgs.

The mass of the SM Higgs is determined in a fit to all available electroweak measurements. As the weak radiative corrections depend quadratically on the mass of the top quark its direct determination at the Tevatron is important for the determination of m_H. This fit yields an estimate for the Higgs mass in the SM and an upper limit [35]:

$$m_\mathrm{H} = 76\,^{+79}_{-45}\ \mathrm{GeV} \qquad m_\mathrm{H} < 220\ \mathrm{GeV}\,. \tag{7}$$

The asymmetric errors reflect the logarithmic dependence of electroweak observables on the Higgs mass. The χ^2 of this fit as function of m_H is shown in Fig.17. The band indicates the estimated theoretical uncertainty which contributes to about ± 5 GeV to the errors of Eq.7. Also shown in Fig.17 is the χ^2 curve when a more theory dependent calculation of the hadronic contribution to the running of the QED coupling constant α is used [36]. The lower limit on m_H obtained from the direct search for the Higgs boson at LEP is shown as a band.

6 Search for Higgs Bosons at LEP

Before the startup of the LEP collider in 1989 experiments were only sensitive to very small Higgs boson masses and the limits derived were subject to large uncertainties [37]. The experiments performed at LEP search for the production of the Higgs boson in electroweak processes which are readily calculable and do not suffer from large theoretical uncertainties. In addition, the LEP collider is a copious source of a heavy particle, the Z boson, which ensures large Higgs production cross sections. For these reasons the LEP experiments have eclipsed previous experimental limits such that at the end of the running at the Z resonance in 1995 the entire mass range for the SM Higgs boson $0 \leq m_\mathrm{H} \leq 63.9$ GeV [38] could be excluded.

With the increase of the cms energy the search for the SM Higgs continues now for larger Higgs mass values. The production of SM Higgs bosons at LEP II would proceed mainly through the Higgs-strahlung diagram shown in Fig.18 with small contributions from WW and ZZ fusion. The range of Higgs masses which can be explored at a given cms energy is then limited by the fact that the Higgs boson is produced in conjunction with a real Z boson. Below this kinematic threshold the cross section $\mathrm{e^+e^-} \rightarrow \mathrm{ZH}$ rises quickly to a sizeable level as compared to other SM processes. This results in a much better signal to background ratio as compared to Higgs searches performed at the Z resonance.

Following the decay modes of the Z and Higgs bosons four final states are distinguished in the search for the Higgs. In the mass range investigated the Higgs decays predominantly into b quarks ($\approx 84\%$), but also its decays into tau leptons and other quarks are considered: (i) $\mathrm{HZ} \rightarrow \mathrm{H\,q\bar{q}}$ (four jets); (ii) $\rightarrow \mathrm{H}\,\nu\bar{\nu}$ (two acoplanar jets); (iii) $\rightarrow \mathrm{H\,e^+e^-}$, $\mathrm{H}\mu^+\mu^-$ (two jets and two leptons) and (iv) $\rightarrow \tau^+\tau^-\,\mathrm{q\bar{q}}$. The main backgrounds are fermion-pair production, in particular $\mathrm{e^+e^-} \rightarrow \mathrm{q\bar{q}}(\gamma)$, four fermion final states from $\mathrm{e^+e^-} \rightarrow \mathrm{W^+W^-}$ and $\mathrm{e^+e^-} \rightarrow \mathrm{ZZ}$ and for $\mathrm{H}\,\nu\bar{\nu}$ the production of single W bosons $\mathrm{e^+e^-} \rightarrow \mathrm{We}\nu$.

The most sensitive channel in the Higgs search is the four-jet topology due to the high hadronic branching ratio of the Z. The tagging of b quarks is essential in all decay channels to suppress background. Kinematic fits are employed to improve the mass resolution on the hypothetical Higgs boson in candidate events. The fits exploit the fact that the two objects, jets or leptons, not associated to the Higgs should stem from a real Z boson.

No indication for Higgs boson production is observed at LEP so far and only lower mass limits can be derived from the negative search results [39–42]. The hypothesis of Higgs boson production, with respect to the presence of background only, is then tested as a function of m_{H} taking into account candidate events and their significance for a given mass value. Fig.19 shows the CL for Higgs production as a function of m_{H} as obtained by ALEPH from which the experimental mass limit is derived. In addition to the measured CL the expected CL is also shown. It is derived from a large number of Monte Carlo experiments simulating the data sample and detector performance in the background-only hypothesis. The results of the SM Higgs boson searches using all data up to $\sqrt{s} = 183$ GeV are published by all four experiments [39–42]. The individual results are combined [43] leading to a lower experimental mass limit of $m_{\mathrm{H}} > 89.7$ GeV.

Preliminary results are now available also from the analysis of the data taken at $\sqrt{s} = 189$ GeV in 1998. When exploring Higgs masses in the vicinity of m_{Z} the production of Z pairs $\mathrm{e^+e^-} \rightarrow \mathrm{ZZ}$, with a cross section an order of magnitude larger than of $\mathrm{e^+e^-} \rightarrow \mathrm{HZ}$, consists an irreducible background. The Z boson has a large branching ratio into b-quarks and due to its natural width and the experimental resolution the mass information does not aid the signal identification. Thanks to the large collected luminosity the cross section $\mathrm{e^+e^-} \rightarrow \mathrm{ZZ}$ is well measured experimentally at this cms energy as well as the background for Higgs boson production. The data do not necessitate an additional contribution from Higgs boson production (Fig.20). Thus masses of the SM Higgs boson close to m_{Z} are excluded by the LEP experiments and lower mass limits up to $m_{\mathrm{H}} > 95$ GeV are obtained [44].

In SUSY models the Higgs sector consists of more than one fundamental scalar particle. At least two Higgs doublets are necessary to create masses for all fermions and their scalar partners. Therefore, in the Minimal Supersymmetric

(MSSM) extension of the SM (see also Sec.7) five Higgs bosons are predicted H^+, H^-, H, h and A, where h is believed to be the lightest one. The charged Higgs bosons are believed to be heavier than the W and beyond the reach of the LEP experiments.

The experiments search for the production of the two additional neutral bosons in the reactions $e^+e^- \rightarrow hA$ and $e^+e^- \rightarrow hZ$. The cross sections of these processes depend on the parameter $\tan\beta$, the ratio of the vacuum expectation values associated to the two Higgs doublets. The production of hA is dominant for large $\tan\beta$ values whereas the reaction $e^+e^- \rightarrow hZ$, with an experimental signature very similar to the SM Higgs production discussed above, governs at low $\tan\beta$.

No evidence for the production of h or A bosons is observed so far at LEP. Lower mass limits are derived for the neutral MSSM Higgs bosons as function of $\tan\beta$. As an example, the preliminary result from OPAL using data up to $\sqrt{s} = 189$ GeV is shown in Fig.21. The limit obtained for small $\tan\beta$ is the same as for the SM Higgs boson and for larger values of $\tan\beta$ masses below 80 GeV are excluded. Also shown in this figure are regions in the plane of $\tan\beta$ and m_{h} which are not allowed by the theory for two different mixing scenarios in the scalar quark sector and for the MSSM parameters assumed to be $m_0 = M_2 = 1$ TeV and $\mu = -100$ GeV. Under these assumptions the LEP experiments start to exclude low values of $\tan\beta$.

The results of the neutral MSSM Higgs boson searches up to $\sqrt{s} = 183\ GeV$ are published [40,42,45,46] and from combining the four experiments [43] lower mass limits of $m_{\mathrm{h}} > 79.6$ GeV and $m_{\mathrm{A}} > 80.2$ GeV are derived for all $\tan\beta$ values. From the preliminary analysis of the data at 189 GeV no evidence is seen for the production of neutral MSSM bosons allowing to exclude them below approximately 84 GeV [44].

Searches for charged Higgs bosons as well as Higgs bosons not decaying in a standard manner are performed by the LEP collaborations without finding any evidence for their existence. Examples of these analyses and results can be found in Ref. [42, 47–52].

7 Search for Supersymmetric Particles at LEP

In addition to the search for the production of SUSY Higgs bosons searches for new particles predicted by SUSY theories [3] have been carried out by the LEP experiments from the Z resonance up to $\sqrt{s} = 189$ GeV. SUSY theories predict the existence of scalar partners of the known quarks, $\tilde{\mathrm{q}}$, and leptons, $\tilde{\ell}^{\pm}$, $\tilde{\nu}$, as well as fermionic partners of the gauge and Higgs bosons. The neutral partners of the bosons mix into four mass eigenstates, called neutralinos, $\tilde{\chi}^0_i$, with the index $i = 1, \ldots, 4$ ordering them by mass. The partner of the charged bosons form two chargino mass eigenstates, the lighter one denoted as $\tilde{\chi}^{\pm}_1$.

Recently published results on searches for charginos, neutralinos, scalar quarks and scalar leptons can be found in Ref. [53–64]. Three different type

Production	Decay
$e^+e^- \to \tilde\chi^0_i\tilde\chi^0_j$	$\tilde\chi^0_i \to \tilde\chi^0_1 f\bar{f},\ \tilde\chi^0_1\gamma \quad (i>1)$
$e^+e^- \to \tilde\chi^+_1\tilde\chi^-_1$	$\tilde\chi^\pm_1 \to \tilde\chi^0_1 q\bar{q},\ \tilde\chi^0_1\ell^\pm\nu,\ \tilde\nu\ell^\pm$
$e^+e^- \to \tilde\ell^+\tilde\ell^-$	$\tilde\ell^\pm \to \tilde\chi^0_1\ell^\pm$
$e^+e^- \to \tilde{q}\,\tilde{q}$	$\tilde{t}_1 \to \tilde\chi^0_1 c,\quad \tilde{b}_1 \to \tilde\chi^0_1 b$

Table 3: Production and decay of SUSY particles as studied by the LEP experiments assuming R-parity conservation.

of models are investigated which can be distinguished by the type and nature of the lightest SUSY particle (LSP): (i) gravity mediated SUSY breaking with a heavy gravitino $\tilde{G}$ and the LSP being the lightest neutralino $\tilde\chi^0_1$; (ii) gauge mediated SUSY breaking with the $\tilde{G}$ as LSP; (iii) R-parity violating SUSY in which the LSP is unstable.

Up to the highest cms energy no sign for SUSY is observed at LEP. A few examples of search results on the first two scenarios are discussed here.

At LEP the production and decay of charginos, neutralinos and scalar leptons and quarks would take place by the reactions listed in Tab.3. The Feynman diagrams contributing to the chargino pair production are shown in Fig.22. With only these assumptions on the production and decay of SUSY particles upper limits on production cross sections are derived from the data.

As an example Fig.23 shows the experimental upper limit on the cross section $e^+e^- \to \tilde\chi^+\tilde\chi^-$ at 189 GeV obtained by OPAL. The most constraining upper limit, $\sigma_{\tilde\chi^+\tilde\chi^-} < 0.07$ pb, is obtained in the region $m_{\tilde\chi^\pm} \approx 80$ GeV and $m_{\tilde\chi^0} \approx 60$ GeV where the kinematic conditions are favourable providing high detection efficiency and good background suppression. Limits on the cross section become worse as the neutralino mass approaches the mass of the chargino because the visible energy in the detector becomes lower and thus reduces the detection efficiency. Also background from two-photon processes is larger there. Similarly, if the mass difference between chargino and neutralino is large the missing energy is reduced and chargino events resemble more and more SM background like W-pair production. This makes background suppression difficult and consequently only higher cross sections can be excluded. Chargino masses below 45 GeV are ruled out by measurements at the Z resonance. The region above the dashed line is kinematically not allowed by requiring that the neutralino is lighter than the chargino. Limits on the pair production cross sections for scalar electrons, muons and taus are shown in Fig.24.

The upper limit on production cross sections on SUSY particles are now interpreted in the framework of the MSSM. The free parameters are the gaugino mass at the weak scale M_2, the mass scale of the scalar partners of the fermions m_0, the mixing parameter of the two Higgs field doublets μ, the trilinear coupling paramter A and $\tan\beta$. Values around $\tan\beta = 1.5$ and 35 are favoured by cosmological arguments.

In the MSSM high cross sections of the order of several picobarn are expected for a wide range of parameter space in the kinematically accessible region at LEP II, in particular for chargino pair production. Expected cross sections at $\sqrt{s} = 189$ GeV as a function of the chargino mass are shown in Fig.25. The two bands shown, obtained from MSSM parameter variations, correspond to a high scalar neutrino mass $m_{\tilde{\nu}}$ and to the lowest mass compatible with the limit obtained at LEP I. The chargino is assumed to be 10 GeV or 3 GeV heavier than the invisible LSP which guarantees that the chargino production could be observed experimentally. The expected cross section depends on $m_{\tilde{\nu}}$ because the t-channel exchange of scalar neutrinos interferes destructively with the s-channel boson exchange and it reaches a minimum for $m_{\tilde{\nu}} \approx 100$ GeV. From the non-observation of a signal upper limits on the chargino production cross section are set and converted into lower mass limits which are in some cases close to the kinematic limit.

Mass limits in the MSSM from the search for scalar leptons are shown in Fig.26 from combining the data of the four experiments up to $\sqrt{s} = 183$ GeV.

Mass limits on scalar top and bottom quarks are presented in Fig.27 as obtained by the DELPHI experiment. Mass eigenstates of scalar top and bottom quarks are superpositions of the scalar partners of the left- and right-handed quarks, e.g. $\tilde{\mathrm{t}}_1 = \tilde{\mathrm{t}}_{\mathrm{L}} \cos\Theta_{\mathrm{LR}} + \tilde{\mathrm{t}}_{\mathrm{R}} \sin\Theta_{\mathrm{LR}}$. The coupling of the $\tilde{\mathrm{t}}_1$ to the Z depends on the mixing angle Θ_{LR} and for a value of $\cos\Theta_{\mathrm{LR}} = 0.57$ the scalar top decouples from the Z leading to a minimal production cross section. In this case the derived mass limit on the scalar top is lower as compared to the case of no mixing, i.e. assuming that the mass eigenstate corresponds to the scalar partner of the left-handed top quark. Similarly, mass limits for a scalar bottom quark are shown for these two scenarios at the bottom of Fig.27. To obtain these limits 100% branching ratios into $\tilde{\mathrm{t}}_1 \to \mathrm{c}\tilde{\chi}^0_1$ and $\tilde{\mathrm{b}}_1 \to \mathrm{b}\tilde{\chi}^0_1$ are assumed.

The results on SUSY searches are often presented in an exclusion plot in the $M_2 - \mu$ parameter plane. Fig.28 shows the result obtained by OPAL based on chargino and neutralino searches for two assumptions on $\tan\beta$.

The lightest neutralino is a candidate for the dark matter in the universe. Therefore, a lower limit on $m_{\tilde{\chi}^0_1}$ valid for all choices of MSSM parameter is particularly interesting. From scanning the MSSM parameter space the LEP experiments obtain values for this absolute limit in the vicinity of 30 GeV, for instance $m_{\tilde{\chi}^0_1} > 27.9$ GeV is obtained by OPAL. This result is illustrated in Fig.29 where the lower mass limit is shown as a function of $\tan\beta$ for all choices of m_0 as well as for high m_0.

Gauge mediated SUSY breaking models in which the gravitino is light can be investigated at LEP by studies of photonic final states. Processes like $\mathrm{e}^+\mathrm{e}^- \to \tilde{\mathrm{G}}\tilde{\mathrm{G}}\gamma$ or $\mathrm{e}^+\mathrm{e}^- \to \tilde{\mathrm{G}}\tilde{\mathrm{G}} \to \tilde{\chi}^0_1\tilde{\chi}^0_1\gamma\gamma$ lead to one or more photons visible in the detector and nothing else. Also in the MSSM production of heavier neutralinos and their subsequent radiative decay would produce this experimental signature. In the SM the reaction $\mathrm{e}^+\mathrm{e}^- \to \nu\bar{\nu}\gamma$ gives rise to observed final states with photons and missing energy.

Fig.30 shows the energy spectrum of single photon events as measured by L3 at $\sqrt{s} = 189$ GeV. Good agreement with the SM expectation is observed, in the total rate as well as in the shape of the distribution.

The study of di-photon events can then be used to set upper limits on the cross section for the process $\mathrm{e^+e^-} \rightarrow \tilde{\chi}_1^0\tilde{\chi}_1^0 \rightarrow \tilde{\mathrm{G}}\tilde{\mathrm{G}}\gamma\gamma$ and to interpret them in terms of mass limits for SUSY particles. The excluded mass of the lightest neutralino as a function of the scalar electron mass is shown in Fig.31. It is compared to the kinematically allowed region of the CDF event [65] which could be explained by production of scalar electrons [66]. Almost the entire region is excluded now by the LEP experiments proving unlikely this explanation of the CDF event.

In SUSY models with a superlight gravitino also the process $\mathrm{e^+e^-} \rightarrow \tilde{\mathrm{G}}\tilde{\mathrm{G}}$ can be relevant and, when accompanied by initial state radiation, modify the observed single photon spectrum. If the mass of the next-to-lightest SUSY particle exceeds the cms energy this is the only accessible reaction to produce SUSY particles [67]. The single photon spectrum observed by DELPHI at $\sqrt{s} = 189$ GeV yields a lower mass limit of $m_{\tilde{\mathrm{G}}} > 9.1 \cdot 10^{-6}$ eV. This corresponds to a lower limit of the SUSY breaking scale of $\sqrt{F} > 193$ GeV.

8 Conclusions and Outlook

The LEP collider and the four experiments have been operated successfully at cms energies from the Z resonance up to 189 GeV. Many precise measurements are performed with the large amount of data collected, for example the determination of the properties of the Z and W bosons. The SM of electroweak and strong interactions is confirmed up to an energy of $\sqrt{s} = 189$ GeV. The search for new physics is extended up to this energy. No sign of Higgs boson production or of SUSY is observed by the experiments. The negative search results for new particles yield many improved lower mass limits.

In the years 1999 and 2000 the energy of the LEP collider will be further increased up to $\sqrt{s} \approx 200$ GeV with the goal of collecting in total 500 pb^{-1} per experiment above the W-pair production threshold. This will allow the more precise determination of W parameters and to extend the kinematic range in the search for new particles. For example the SM Higgs boson could be discovered up to a mass of $m_{\mathrm{H}} \approx 105$ GeV.

9 Acknowledgements

I would like to thank the organisers of the ITEP winter school for their hospitality. Many colleagues from the LEP experiments helped me to compile the results from the recent run. Also, I am grateful to M. von der Mey and M. Weber for the careful reading of the manuscript.

References

[1] S.L. Glashow, Nucl. Phys. **22** (1961) 579;
S. Weinberg, Phys. Rev. Lett. **19** (1967) 1264;
A. Salam, "Elementary Particle Theory", Ed. N. Svartholm, Stockholm, "Almquist and Wiksell" (1968), 367.

[2] P.W. Higgs, Phys. Lett. **B 12** (1964)132;
F. Englert and R. Brout, Phys. Rev. Lett. **13** (1964) 321;
G.S. Guralnik et al., Phys. Rev. Lett. **13** (1964) 585.

[3] P. Fayet, Phys. Lett. **B 64** (1976) 156, Phys. Lett. **B 69** (1977) 489;
P. Fayet and S. Ferrara, Phys. Rep. **32** (1977) 249;
H.P. Nilles, Phys. Rep. **110** (1984) 1;
H. Haber and G. Kane, Phys. Rep. **117** (1985) 75.

[4] "Z Physics at LEP I", CERN Report CERN 89-08 (1989), eds. G. Altarelli, R. Kleiss and C. Verzegnassi.

[5] The LEP Coll. ALEPH, DELPHI, L3, OPAL, the LEP Electroweak Working Group and the SLD Heavy Flavour Group, Preprint CERN-EP/99-054, CERN, 1999.

[6] R. Assmann et al., E. Phys. J. **C 12** (1999) 187.

[7] D. Bardin et al., FORTRAN package ZFITTER, Preprint CERN-TH 6443/92;
D. Bardin et al., Z. Phys. **C 44** (1989) 493;
D. Bardin et al., Nucl. Phys. **B 351** (1991) 1;
D. Bardin et al., Phys. Lett. **B 255** (1991) 290.

[8] G. Montagna et al., Nucl. Phys. **B 401** (1993) 3;
G. Montagna et al., Comp. Phys. Comm. **76** (1993) 328.

[9] ALEPH Coll., R. Barate et al., Study of Fermion pair production in e^+e^- collisions at $130 - 183$ GeV, Preprint CERN-EP/99-042, CERN, 1999, submitted to E. Phys. J.

[10] DELPHI Coll., P. Abreu et al., Measurement and Interpretation of Fermion-Pair Production at LEP energies from 130 to 172 GeV, Preprint CERN-EP/99-005, CERN, 1999, submitted to E. Phys. J.

[11] L3 Collab., M. Acciarri et al., Phys. Lett. **B 407** (1997) 361.

[12] OPAL Coll., K. Ackerstaff et al., E. Phys. J. **C 6** (1999) 1.

[13] E. Eichten, K. Lane and M. Peskin, Phys. Rev. Lett. **50** (1983) 81.

[14] S. Wynhoff, “Measurement of Fermion Pair Production at LEP2”, presentation at the ICHEP 98 conference, Vancouver (1998), to appear in the proceedings.

[15] L3 Collab., M. Acciarri et al., Phys. Lett. **B 444** (1998) 569.

[16] ALEPH Coll., R. Barate et al., Phys. Lett. **B 453** (1999) 107.

[17] DELPHI Coll., P. Abreu et al., W pair production cross section and W branching fractions in e^+e^- collsions at 183 GeV, Preprint CERN-EP/99-047, CERN, 1999, submitted to Phys. Lett. B.

[18] L3 Collab., M. Acciarri et al., Phys. Lett. **B 436** (1998) 437.

[19] OPAL Coll., G. Abbiendi et al., E. Phys. J. **C 8** (1999) 191.

[20] F. Cavallari, “W,Z Couplings and Cross Sections at LEP II”, presentation at the XXIV Rencontres de Moriond, Les Arcs, France (1999), to appear in the proceedings.

[21] N. Cabbibo, Phys. Rev. Lett. **10** (1963) 531.

[22] M. Kobayashi and M. Maskawa, Prog. Theor. Phys. **49** (1963) 652.

[23] “The 1998 Review of Particle Physics”, C. Caso et al., E. Phys. J. **C 3** (1998) 1.

[24] G. Gounaris, J.L. Kneur and D. Zeppenfeld in “Physics at LEP2”, CERN Report 96-01, eds. G. Altarelli, T. Sjöstrand and F. Zwirner.

[25] ALEPH Coll., R. Barate et al., Phys. Lett. **B 453** (1999) 121.

[26] DELPHI Coll., P. Abreu et al., E. Phys. J. **C 2** (1998) 581.

[27] L3 Collab., M. Acciarri et al., Measurement of Mass and Width of the W Boson at LEP, Preprint CERN-EP/99-017, CERN, 1999, submitted to Phys. Lett. B.

[28] OPAL Coll., G. Abbiendi et al., Measurement of the W Mass and Width in e^+e^- Collsions at 183 GeV, Preprint CERN-EP/98-197, CERN, 1998, submitted to Phys. Lett. B.

[29] M. Hapke, “QCD at LEP II and WW Interactions”, presentation at the XXIV Rencontres de Moriond, Les Arcs, France (1999), to appear in the proceedings.

[30] I. Riu,“ W Mass and LEP Energy Calibration”, presentation at the XXIV Rencontres de Moriond, Les Arcs, France (1999), to appear in the proceedings.

[31] M. Veltman, Nucl. Phys. **B 123** (1977) 89;
M.S. Chanowitz et al., Phys. Lett. **B 78** (1978) 1;
M. Consoli, S. Lo Presti, L. Maiani, Nucl. Phys. **B 223** (1983) 474;
J. Fleischer, F. Jegerlehner, Nucl. Phys. **B 228** (1983) 1.

[32] A. Sirlin, Phys. Rev. **D 22** (1980) 971, Phys. Rev. **D 29** (1984) 89;
W.J. Marciano and A. Sirlin, Phys. Rev. **D 29** (1984) 945.

[33] S. Eidelman and F. Jegerlehner, Z. Phys. **C 67** (1995) 585.

[34] CDF Coll., F. Abe et al., Phys. Rev. Lett. **74** (1995) 2626;
CDF Coll., F. Abe et al., "Measurement of the Top Quark Mass", Preprint hep-ex/9801014, 1998;
D0 Coll., S. Abachi et al., Phys. Rev. Lett. **74** (1995) 2632.

[35] The LEP Coll. ALEPH, DELPHI, L3, OPAL, the LEP Electroweak Working Group and the SLD Heavy Flavour Group, Compilation of results for the 1999 spring conferences, internet: http://www.cern.ch/LEPEWWG/.

[36] M. Davier and A. Höcker, Preprint LAL 97-85, LAL, 1997.

[37] "The 1988 Review of Particle Physics", M. Aiguilar-Benitez et al., Phys. Lett. **B 204** (1988) 1.

[38] S. Park, in 10th Topical Workshop of Proton-Antiproton Collider Physics, eds. R. Raja and G. Yoh, AIP Press, New York 1995.

[39] ALEPH Coll., R. Barate et al., Phys. Lett. **B 447** (1999) 336.

[40] DELPHI Coll., P. Abreu et al., Search for neutral Higgs bosons in e^+e^- collsions at $\sqrt{s}$ = 183 GeV, Preprint CERN-EP/99-006, CERN, 1999, submitted to E. Phys. J..

[41] L3 Coll., M. Acciarri et al., Phys. Lett. **B 431** (1998) 437.

[42] OPAL Coll., G. Abbiendi et al., E. Phys. J. **C 7** (1999) 407.

[43] The LEP Working Group for Higgs Boson Searches ALEPH, DELPHI, L3 and OPAL, Preprint CERN-EP/99-060, CERN, 1999.

[44] M. Felcini, "Higgs and SUSY Searches", presentation at the XXIV Rencontres de Moriond, Les Arcs, France (1999), to appear in the proceedings.

[45] ALEPH Coll., R. Barate et al., Phys. Lett. **B 440** (1998) 419.

[46] L3 Coll., M. Acciarri et al., Phys. Lett. **B 436** (1998) 389.

[47] ALEPH Coll., R. Barate et al., Phys. Lett. **B 450** (1999) 467.

[48] L3 Collab., M. Acciarri et al., Phys. Lett. **B 446** (1999) 368.

[49] ALEPH Coll., R. Barate et al., Phys. Lett. **B 450** (1999) 301.

[50] DELPHI Coll., P. Abreu et al., A search for invisible Higgs bosons produced in e^+e^- interactions at LEP 2 energies, Preprint CERN-EP/99-059, CERN, 1999, submitted to Phys. Lett. B.

[51] DELPHI Coll., P. Abreu et al., Search for the Higgs boson in events with isolated photons at LEP 2, Preprint CERN-EP/99-058, CERN, 1999, submitted to Phys. Lett. B.

[52] OPAL Coll., K. Ackerstaff et al., Phys. Lett. **B 437** (1998) 218.

[53] ALEPH Coll., R. Barate et al., Search for charginos and neutralinos in e^+e^- collisions at centre-of-mass energies near 183 GeV and constraints on the MSSM parameter space, Preprint CERN-EP/99-014, CERN, 1999, submitted to E. Phys. J.

[54] ALEPH Coll., R. Barate et al., Phys. Lett. **B 433** (1998) 176.

[55] ALEPH Coll., R. Barate et al., Phys. Lett. **B 434** (1998) 189.

[56] DELPHI Coll., P. Abreu et al., Search for charginos nearly mass-degenerate with the lightest neutralino, Preprint CERN-EP/99-037, CERN, 1999, submitted to E. Phys. J.

[57] DELPHI Coll., P. Abreu et al., Phys. Lett. **B 446** (1999) 75.

[58] DELPHI Coll., P. Abreu et al., E. Phys. J. **C 6** (1999) 385.

[59] L3 Collab., M. Acciarri et al., Search for R-parity Violating Chargino and Neutralino Decays in e^+e^- Collisions up to $\sqrt{s} = 183$ GeV, Preprint CERN-EP/99-023, CERN, 1999, submitted to Phys. Lett. B.

[60] L3 Collab., M. Acciarri et al., Search for Scalar Leptons in e^+e^- Collisions at $\sqrt{s} = 183$ GeV, Preprint CERN-EP/99-024, CERN, 1999, submitted to Phys. Lett. B.

[61] L3 Collab., M. Acciarri et al., Phys. Lett. **B 445** (1999) 428.

[62] OPAL Coll., G. Abbiendi et al., Search for R-parity Violating Decays of Scalar Fermions at LEP, Preprint CERN-EP/99-043, CERN, 1999, submitted to E. Phys. J.

[63] OPAL Coll., G. Abbiendi et al., Search for Scalar Top and Scalar Bottom Quarks at $\sqrt{s} = 189$ GeV at LEP, Preprint CERN-EP/99-036, CERN, 1999, submitted to Phys. Lett. B.

[64] OPAL Coll., G. Abbiendi et al., E. Phys. J. **C 8** (1998) 255.

[65] CDF Collab., F. Abe et al., Phys. Rev. Lett. **81** (1998) 1791.

[66] J.L. Lopez and D.V. Nanopoulos, Phys. Rev. **D 55** (1997) 4450.

[67] A. Brignole, F. Feruglio and F. Zwirner, Preprint CERN-TH/97-339, CERN, 1997.

[68] CCFR/NuTeV Coll., K. McFarland et al., E. Phys. J. **C 1** (1998) 509; NuTeV Coll., K. McFarland, talk presented at the XXXIIIth Rencontres de Moriond, 1998. hep-ex/9806013.

List of Figures

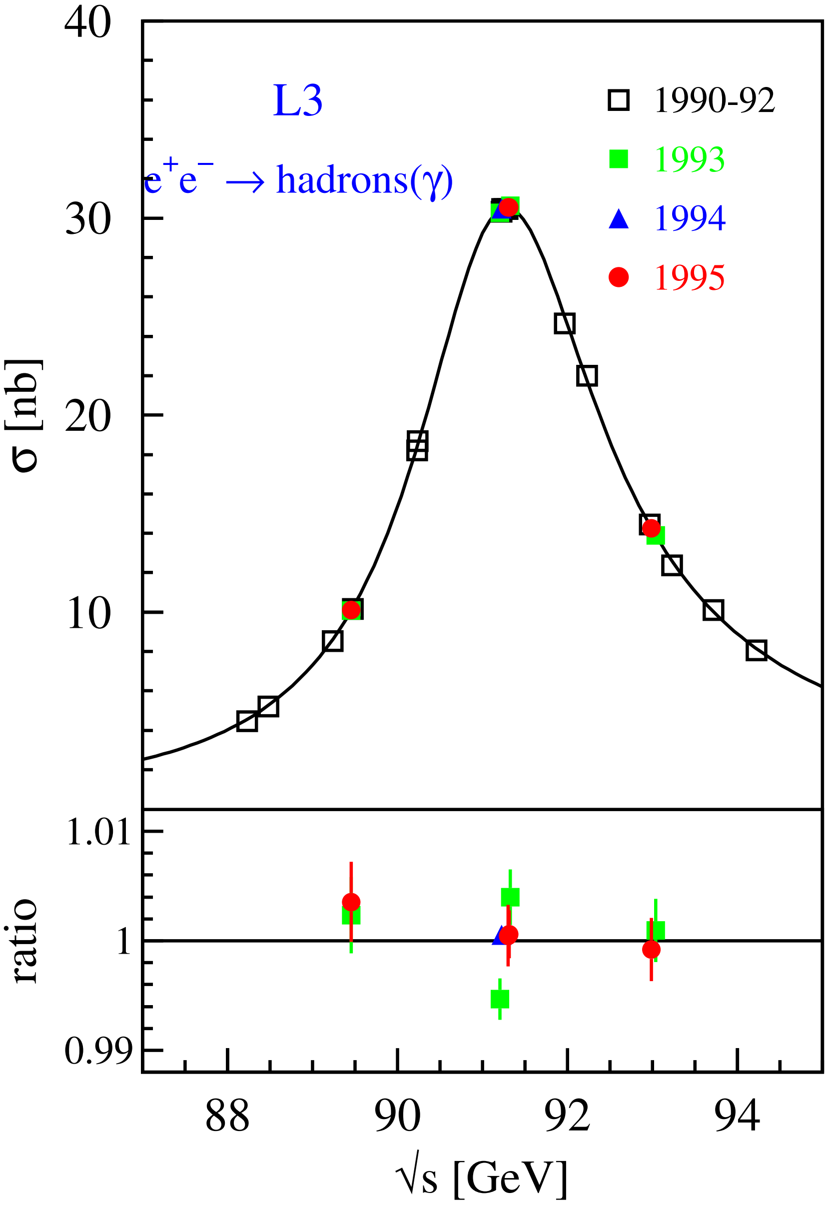

Figure 1: The measured cross section $e^+e^- \to \text{hadrons}(\gamma)$ at the Z resonance compared to the result of a fit for Z parameters. At the bottom the ratio between the measurements with their statistical errors and the result of the fit is shown.

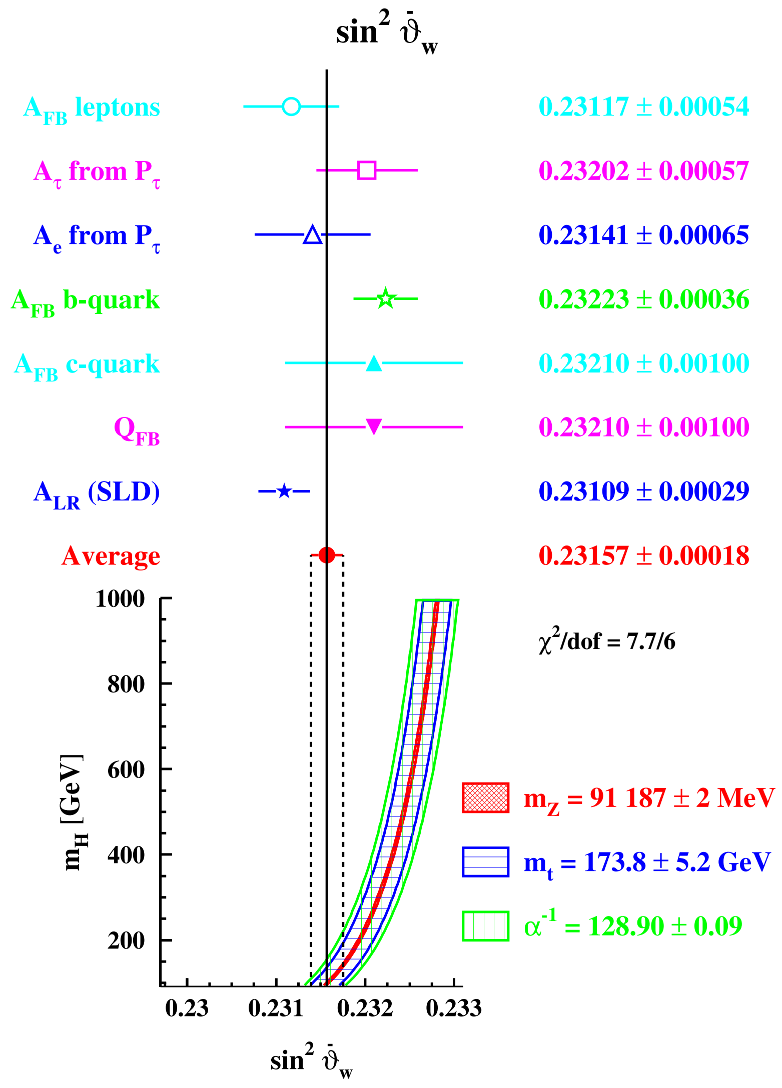

Figure 2: Comparison of measurements of the effective weak mixing angle $\sin^2\bar{\vartheta}_{\rm W}$ from different observables at LEP and by SLD. The measurements are compared to the SM expectation as a function of the Higgs mass.

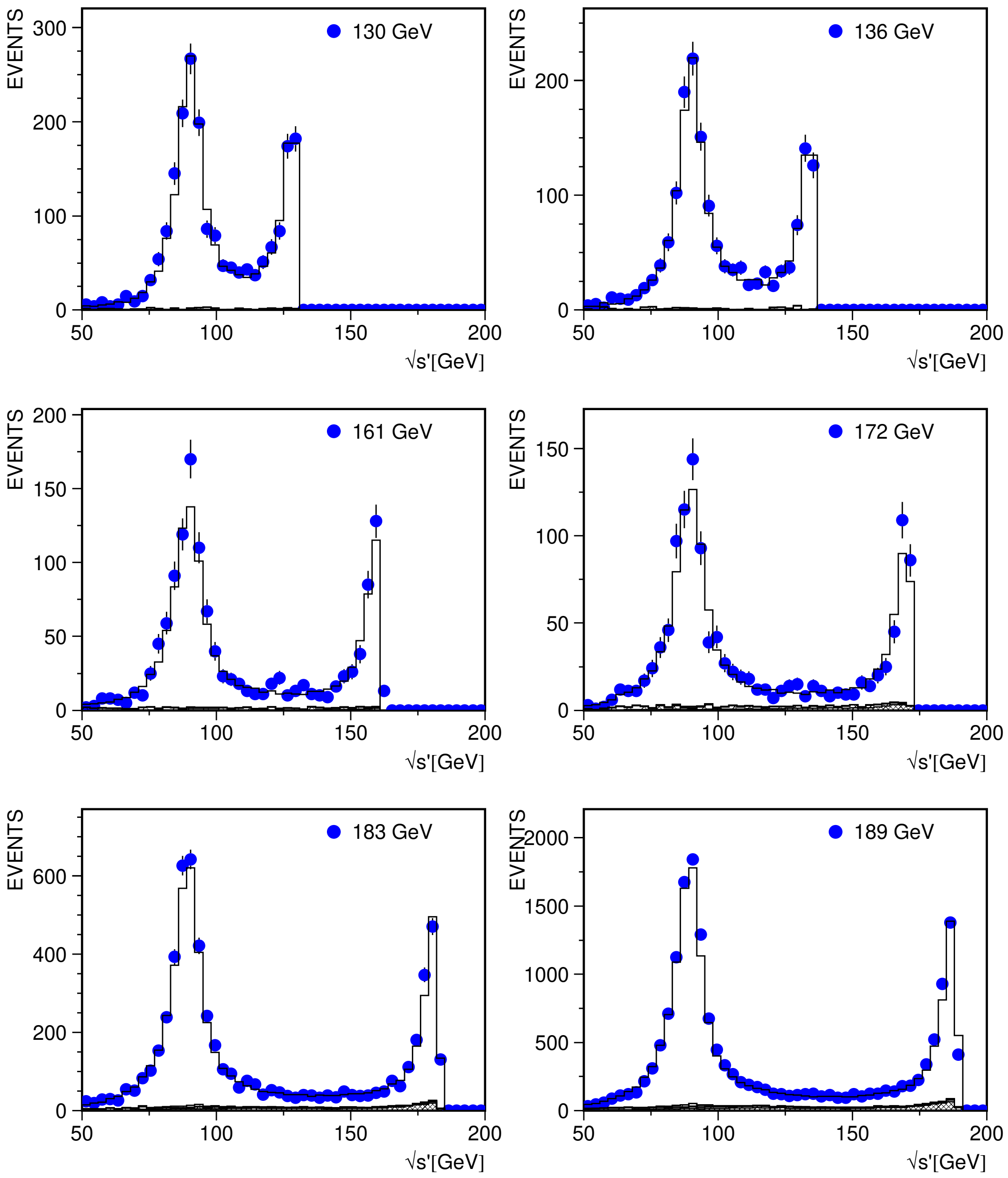

Figure 3: Distribution of the effective cms energy, $\sqrt{s'}$, in the reaction $\mathrm{e^+e^-} \rightarrow$ hadrons(γ) at various cms energies above the Z resonance. The points are the data and the histograms are obtained from Monte Carlo simulations.

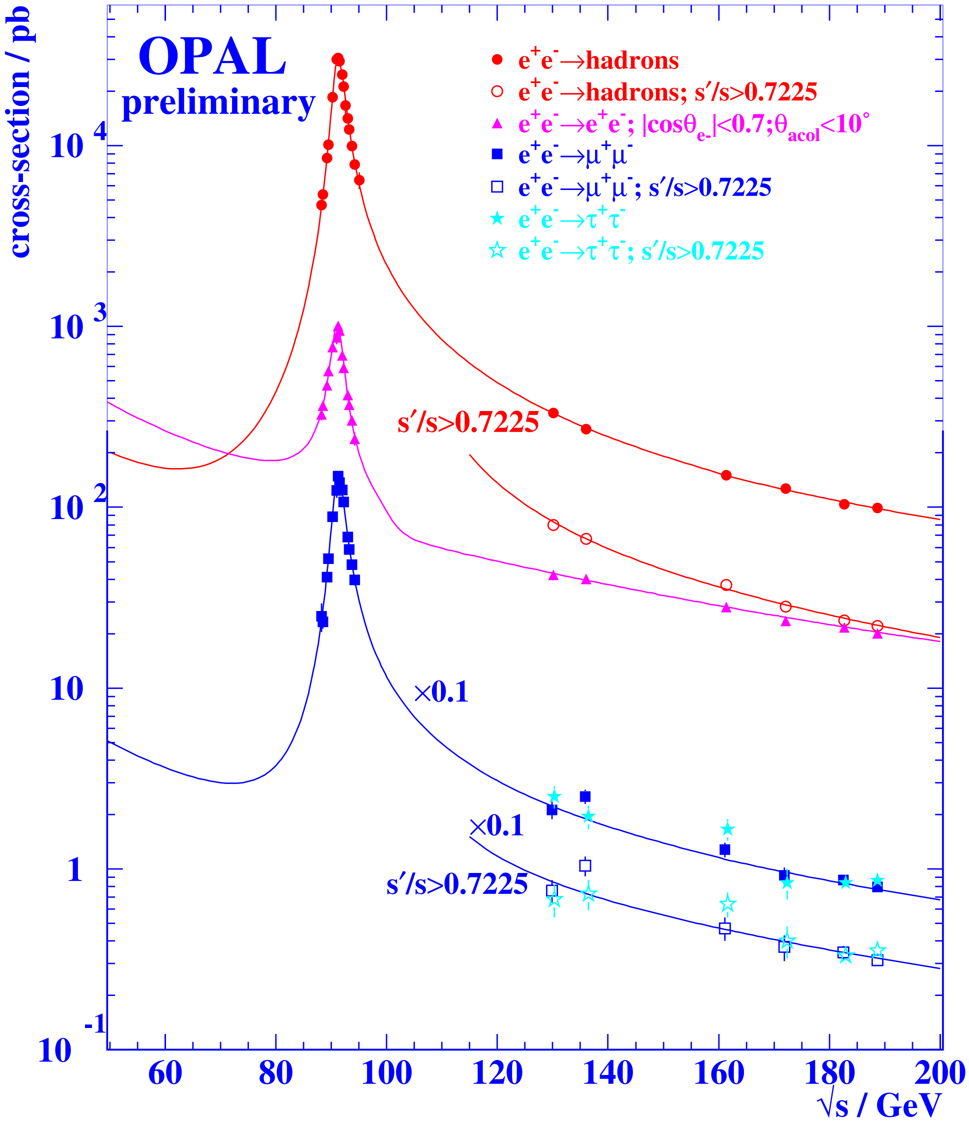

Figure 4: Measured cross sections $e^+e^- \to f\bar{f}(\gamma)$ as function of the cms energy and compared to the SM expectation.

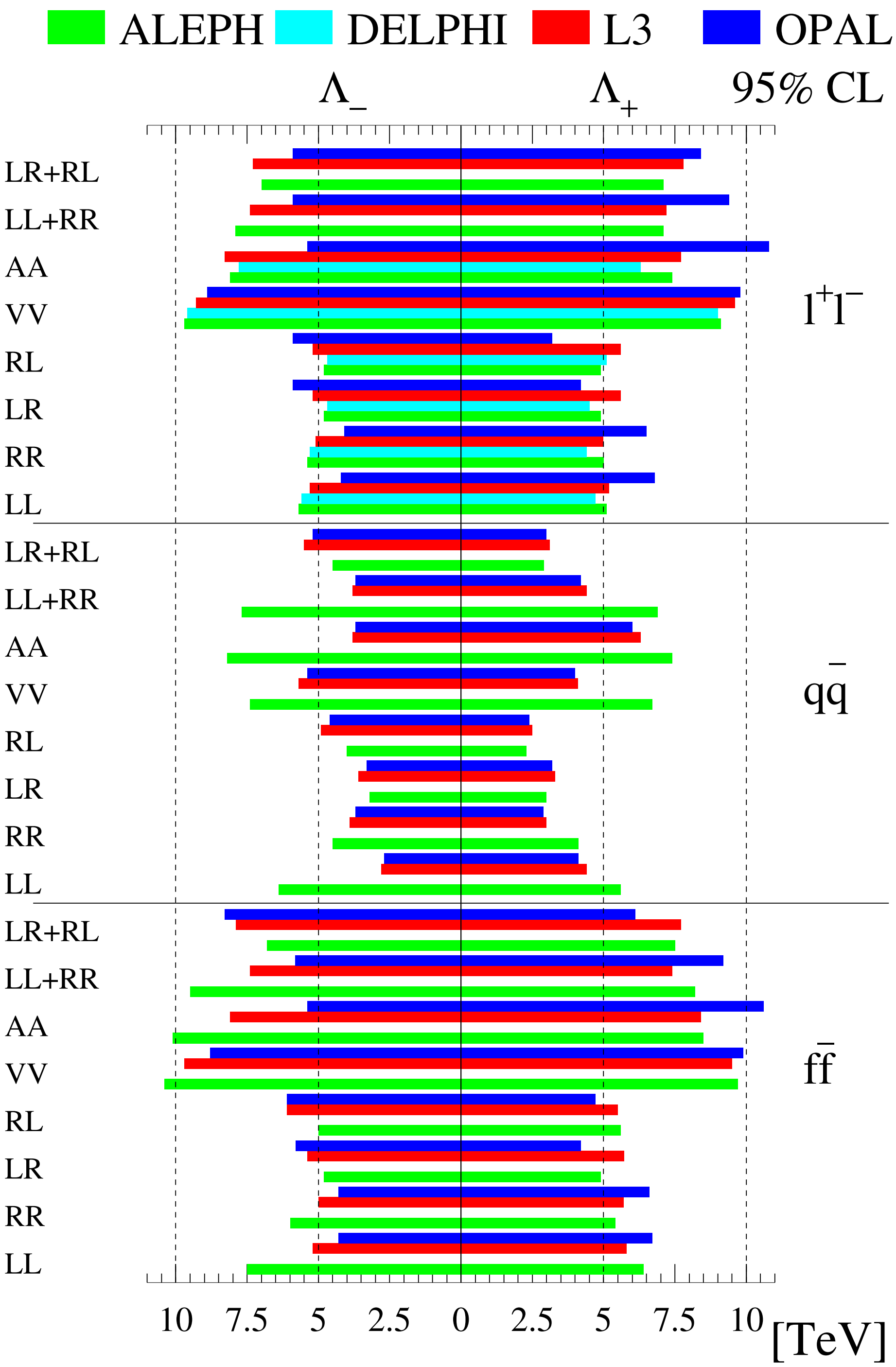

Figure 5: Limits on the energy scale for contact interactions in different scenarios as derived from the measurements of hadronic and leptonic cross sections and forward-backward asymmetries at LEP.

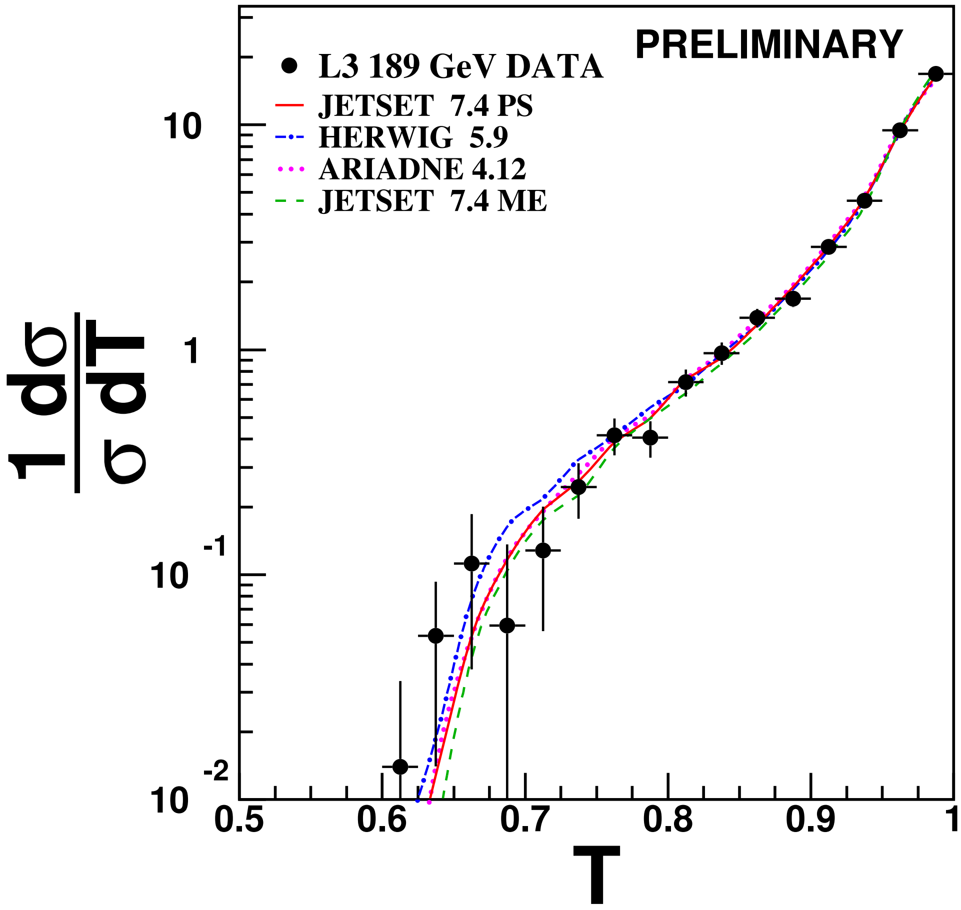

Figure 6: The distribution of thrust in $e^+e^- \to$ hadrons(γ) events at $\sqrt{s}$ = 189 GeV as measured by the L3 experiment compared to Monte Carlo simulations.

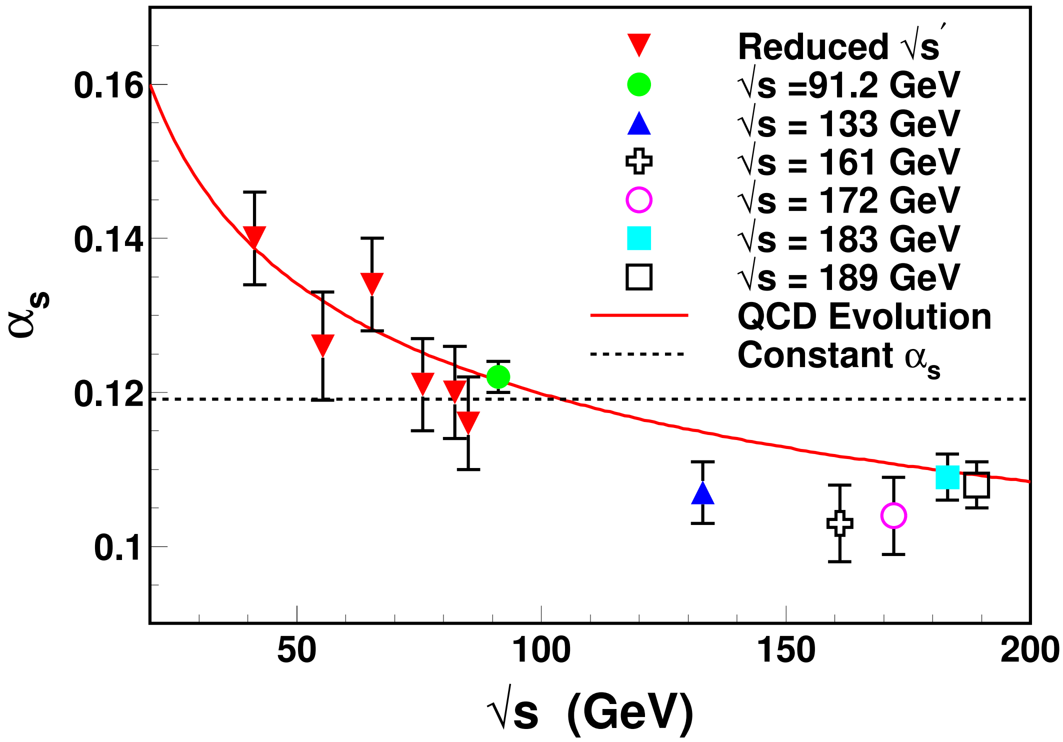

Figure 7: The evolution of the strong coupling constant α_s with energy as measured with the same set of hadronic event shape variables in $e^+e^- \rightarrow$ hadrons(γ).

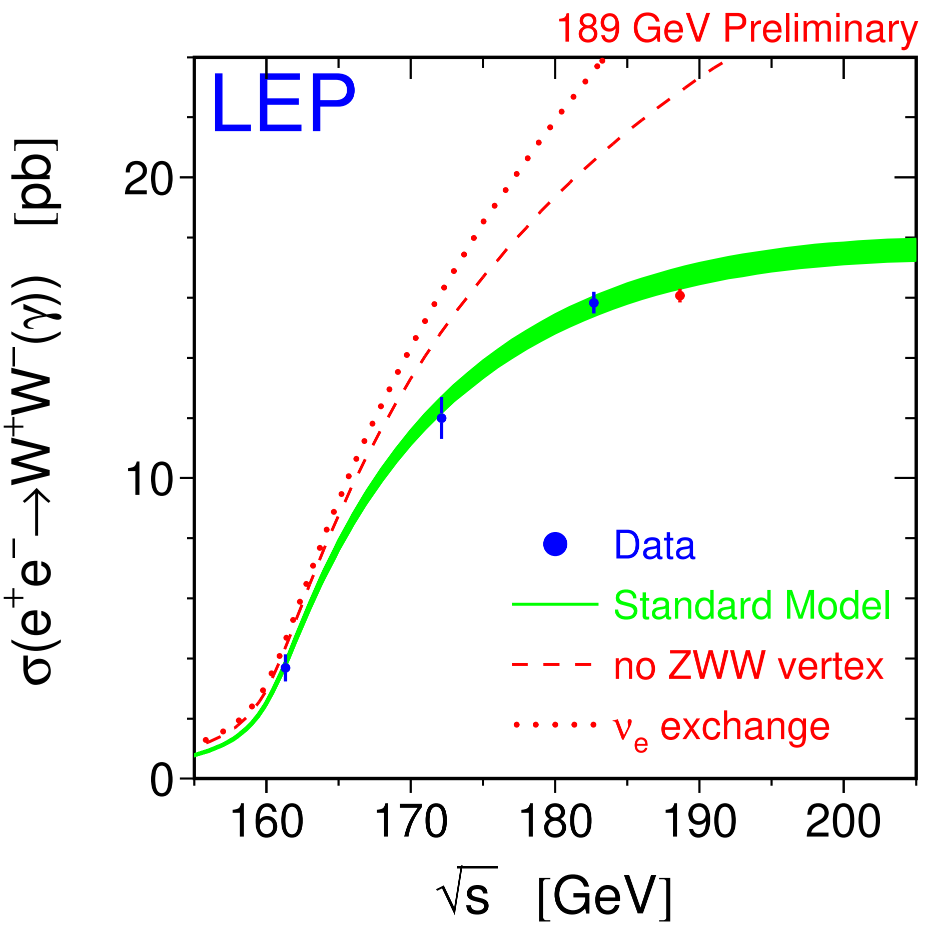

Figure 8: The cross section $e^+e^- \to W^+W^-(\gamma)$ as a function of the cms energy. The combined LEP measurements are compared to the SM prediction (band including theoretical uncertainty) and hypotheses without triple gauge boson couplings.

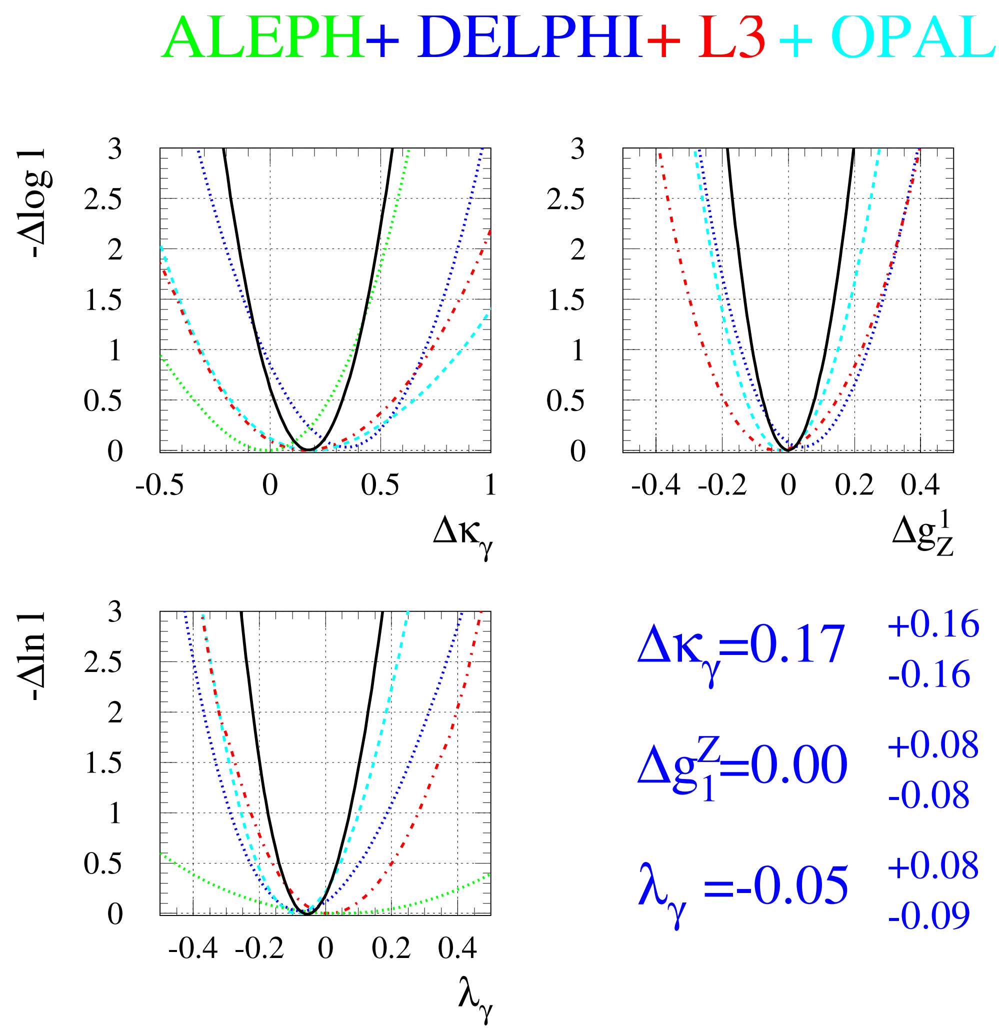

Figure 9: Likelihood curves obtained from the fit for W coupling parameters $\Delta\kappa_\gamma = \kappa_\gamma - 1$, $\Delta g_1^Z = g_1^Z - 1$ and λ_γ by the four experiments and the combined results (solid lines). The central values and errors of the combined result are listed in the right bottom corner.

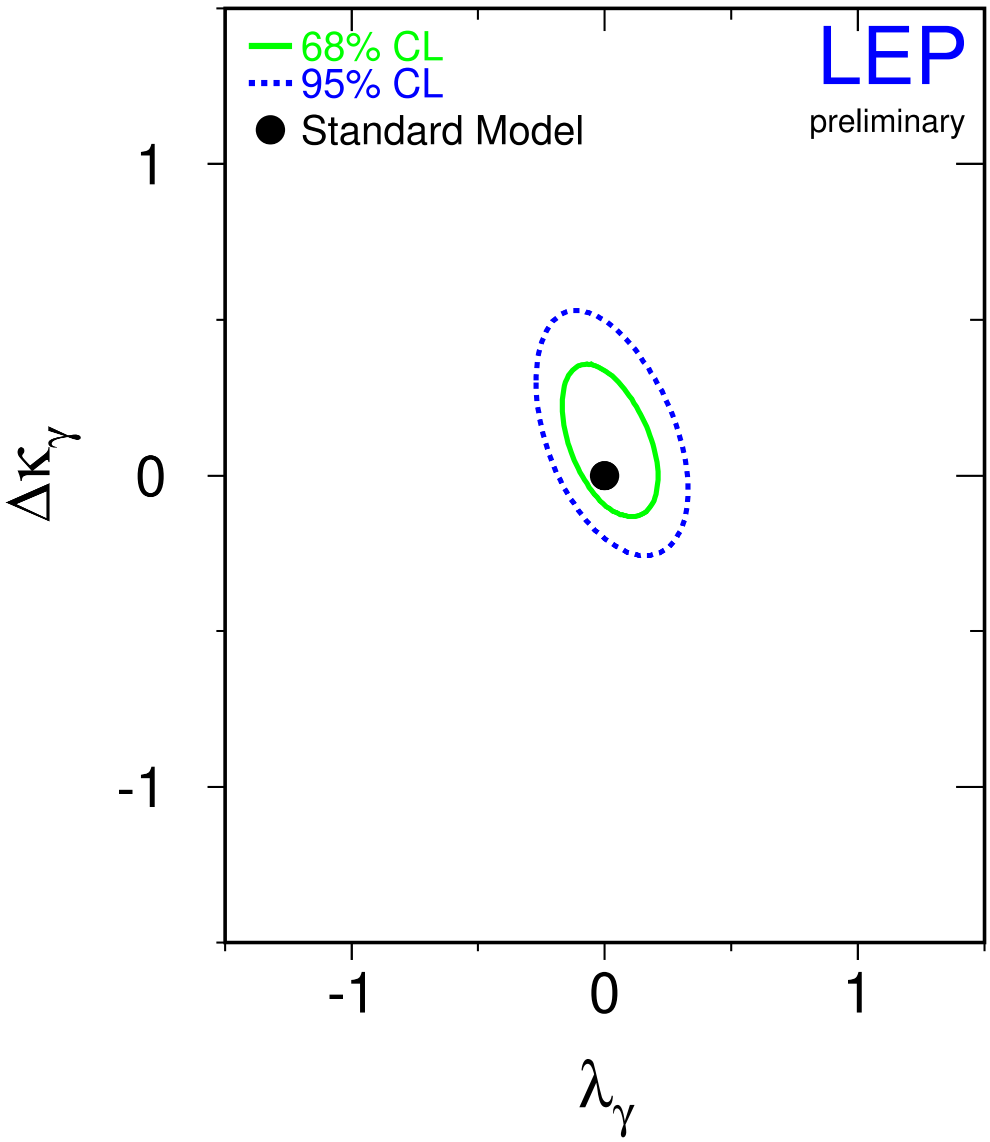

Figure 10: Two parameter fit for W couplings, $\Delta\kappa_\gamma = \kappa_\gamma - 1$ and λ_γ, combining the results of the four experiments.

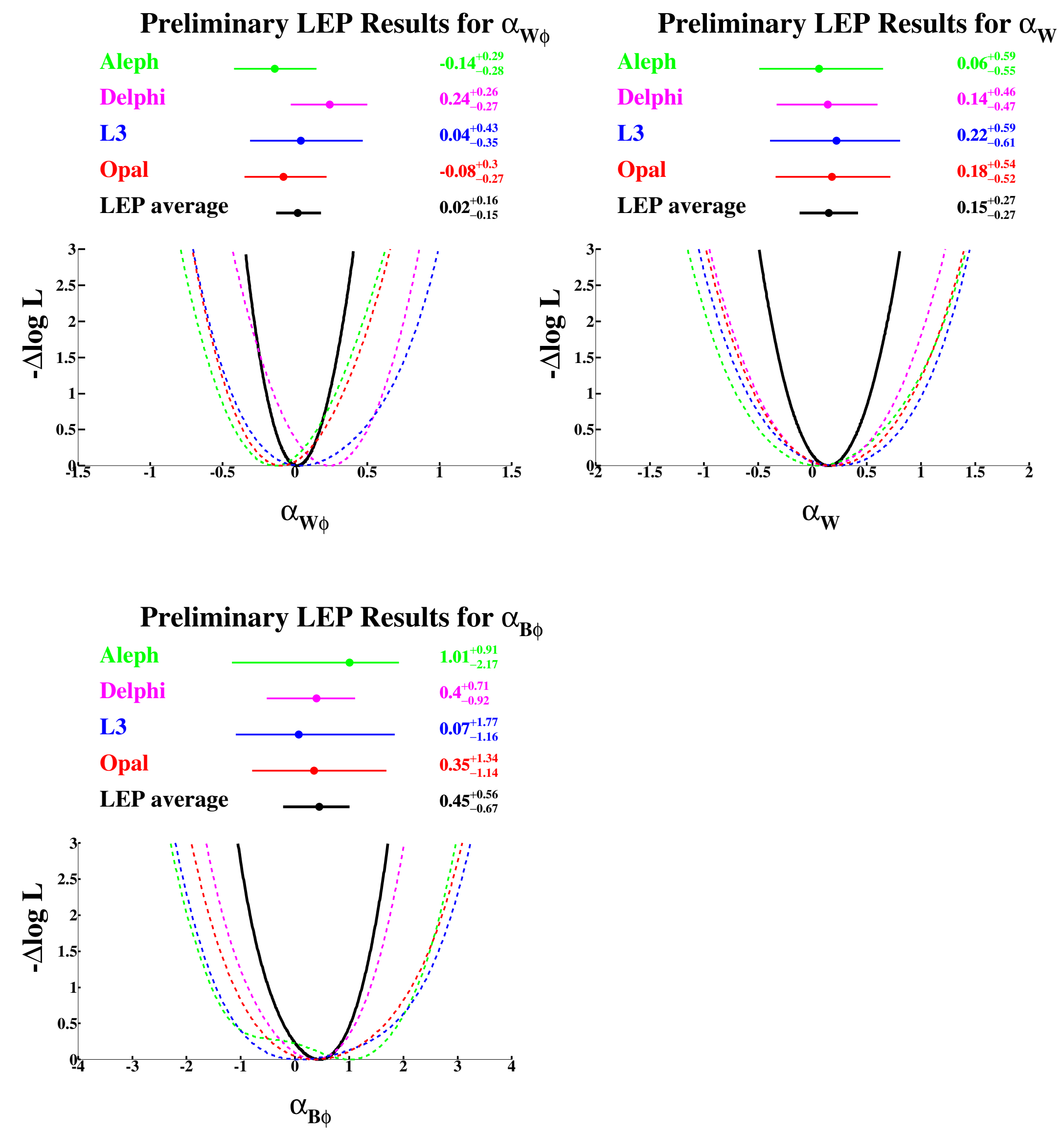

Figure 11: Results and likelihood curves obtained from the fit for the W coupling parameters $\alpha_{W\phi}$, α_{W} and $\alpha_{B\phi}$ by the four experiments and the combined results.

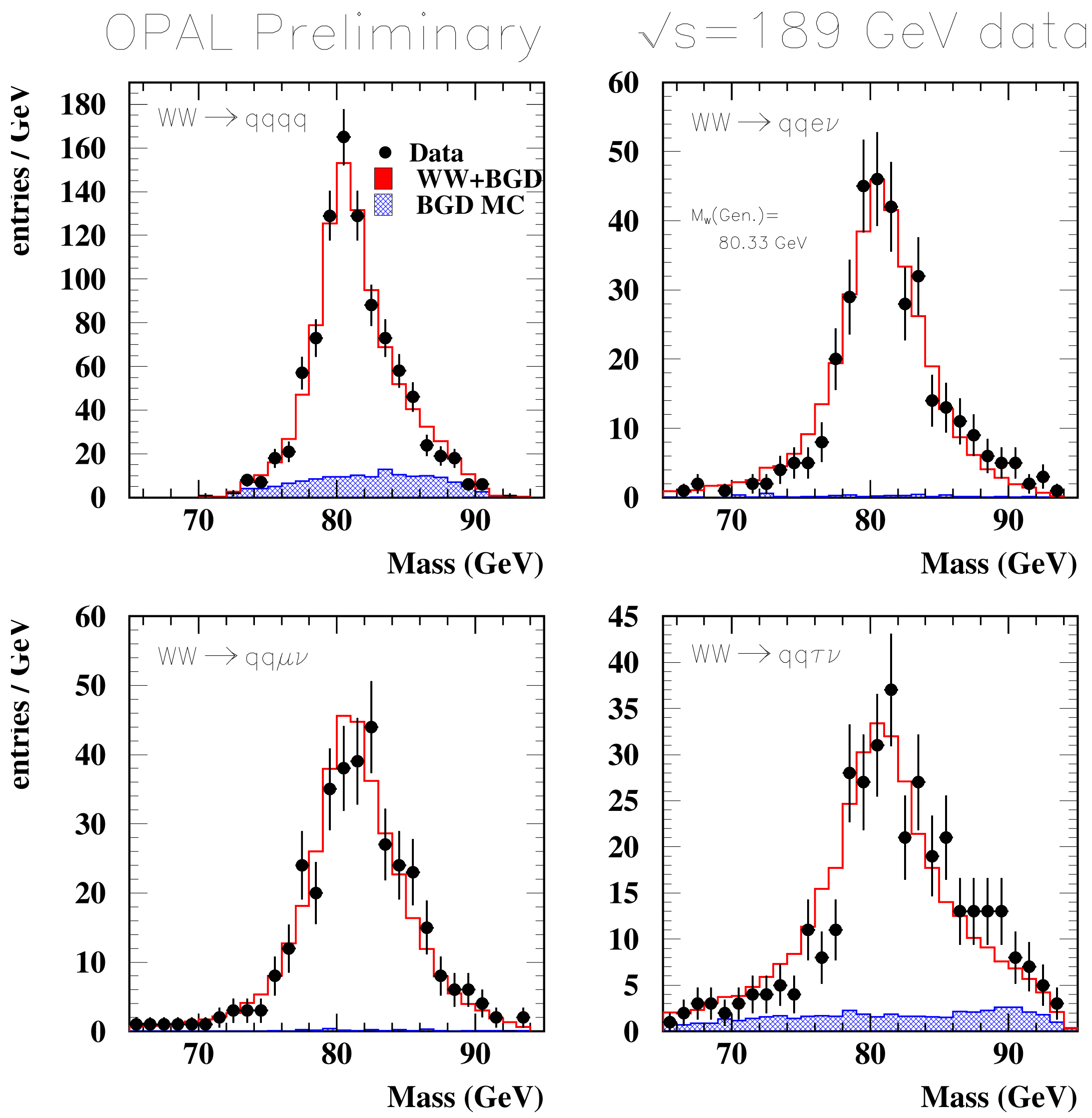

Figure 12: Distributions of the reconstructed W mass obtained by OPAL from the data at $\sqrt{s} = 189$ GeV for four different final states.

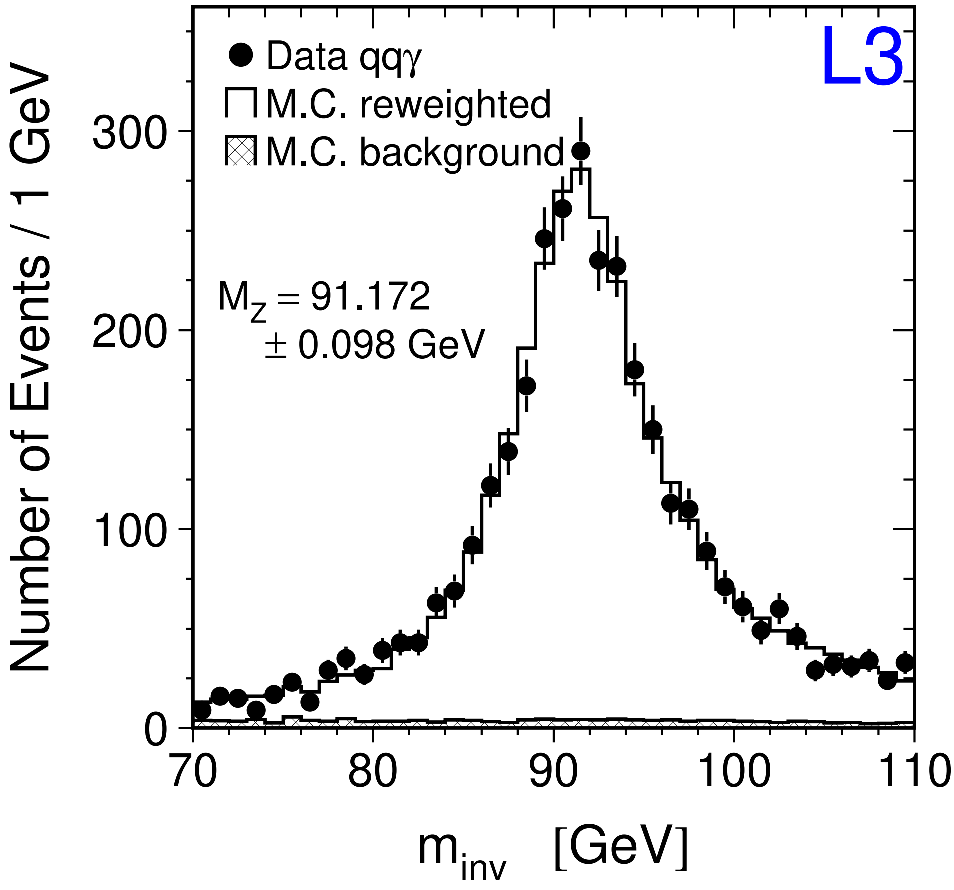

Figure 13: Verification of the method to determine the W mass. Hadronic return-to-the-Z events at $\sqrt{s} = 183$ GeV are used to measure the Z mass from direct reconstruction of the decay products.

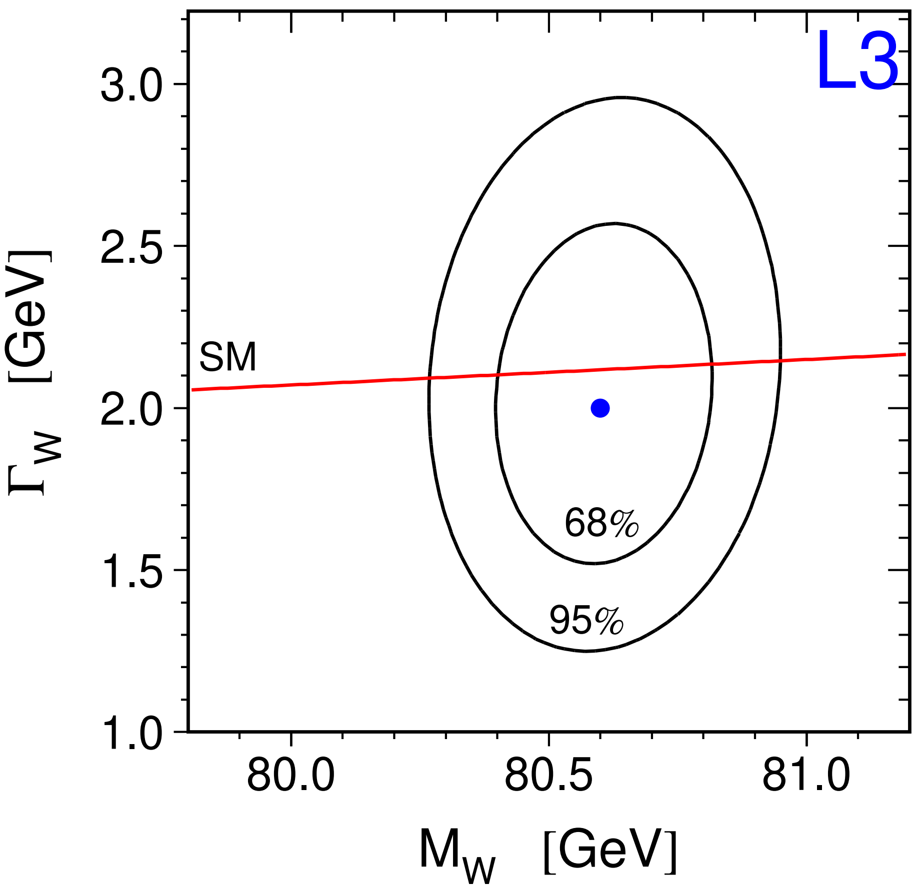

Figure 14: Result of a fit for the W mass and total width from the measured invariant mass distributions using data up to $\sqrt{s} = 183$ GeV.

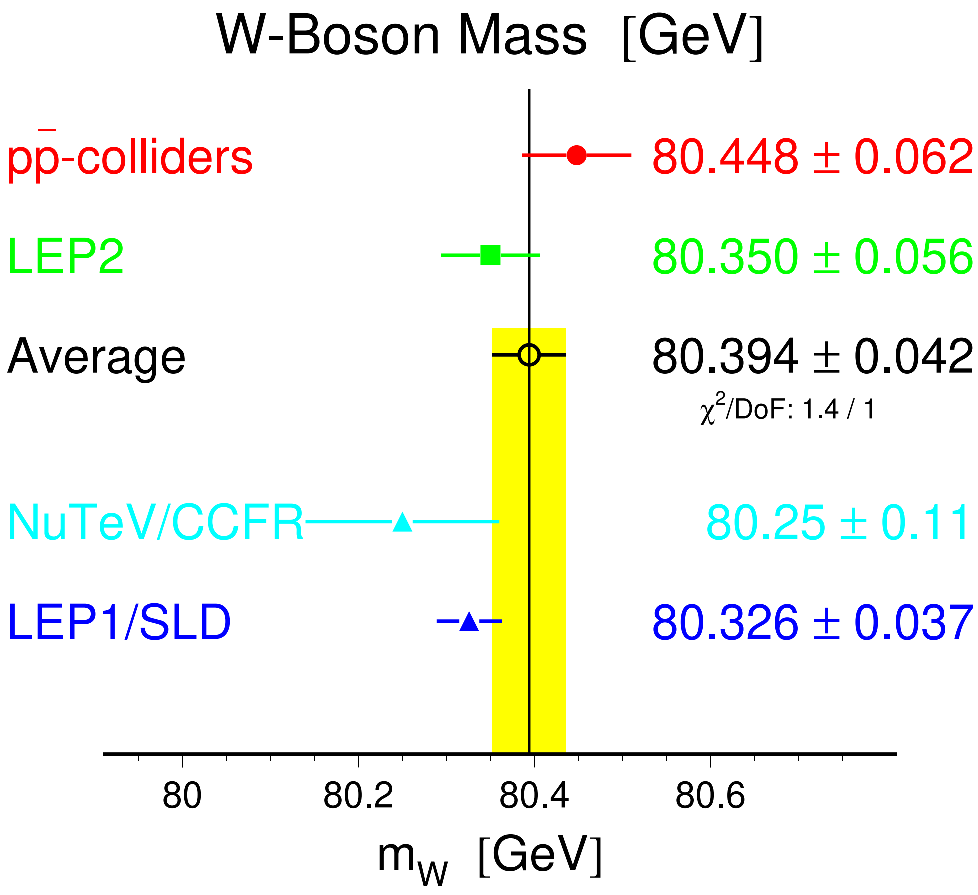

Figure 15: Comparison of different determinations of the mass of the W boson: At the top the results from p$\bar{\text{p}}$-colliders and LEP II are listed, together with their average, as obtained from the reconstruction of W decay products. At bottom W masses are shown as derived from the measurement of $\sin^2\vartheta_W$ in ν-scattering [68] and from precision measurements of observables at the Z resonance by LEP and the SLD experiments.

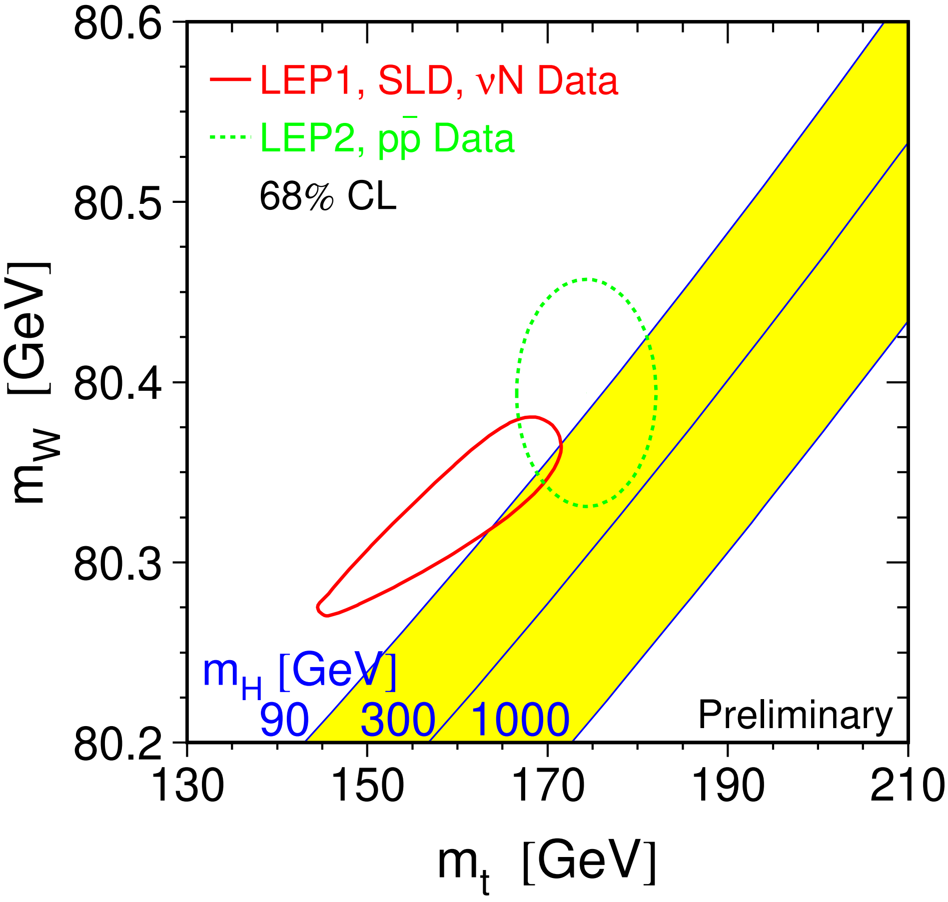

Figure 16: Comparison of indirect and direct determinations of the W boson and top quark masses: The solid contour describes the region in the $m_W - m_t$ plane derived from measurements at the Z resonance and from ν scattering data. The dashed contour is obtained from the direct measurements of these particle masses. The band indicates the SM relation between m_W and m_t (Eq.6) for Higgs boson masses ranging between the lower experimental and the upper theoretical boundaries.

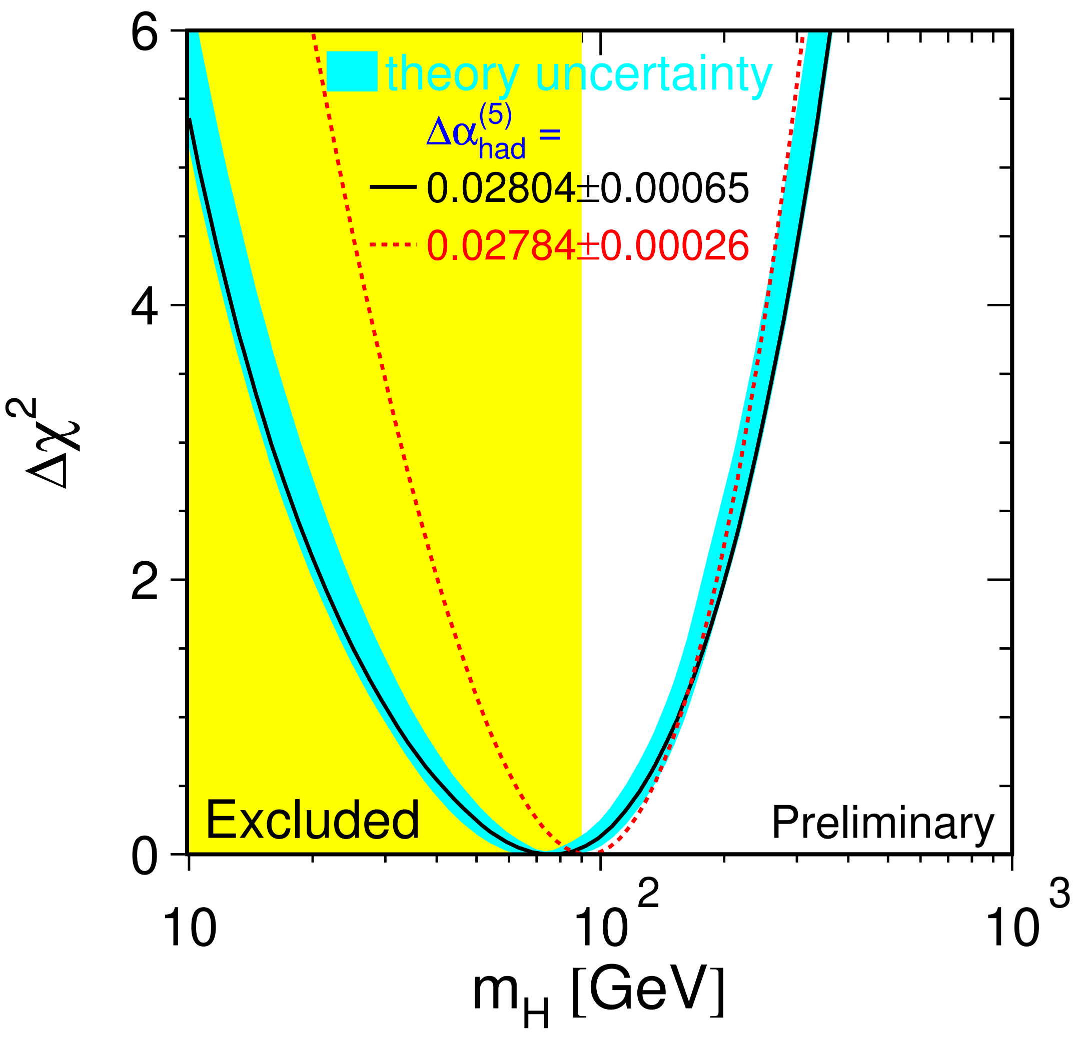

Figure 17: Result of the SM fit for the Higgs mass using all experimental results on electroweak observables.

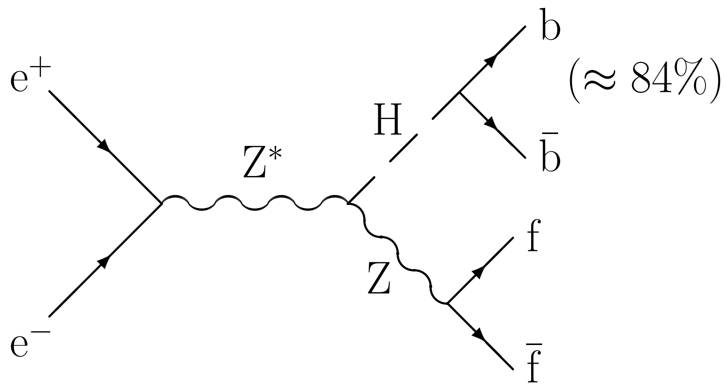

Figure 18: Feynman diagram of the Higgs-strahlung process which would be the main production mechanism for the SM Higgs at LEP II.

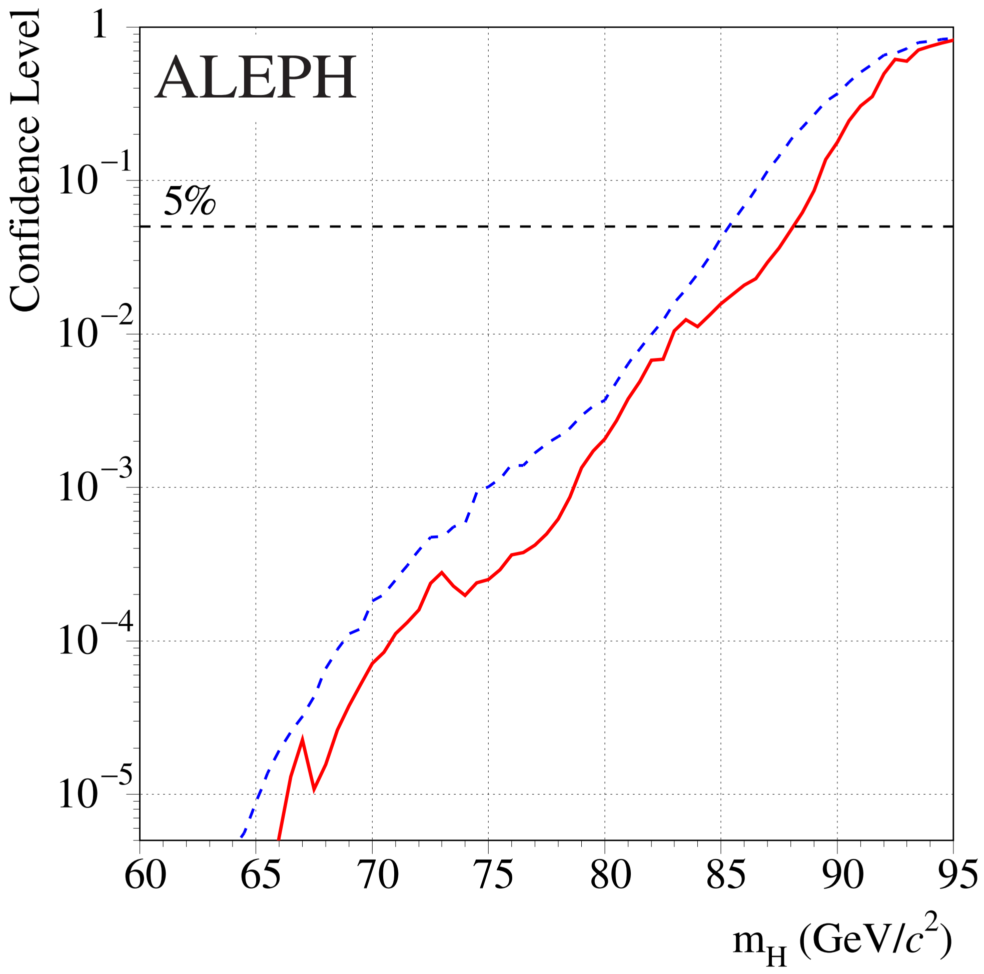

Figure 19: The observed (solid line) and expected (dashed line) confidence level as function of the SM Higgs mass obtained by the ALEPH collaboration using data up to $\sqrt{s} = 183$ GeV.

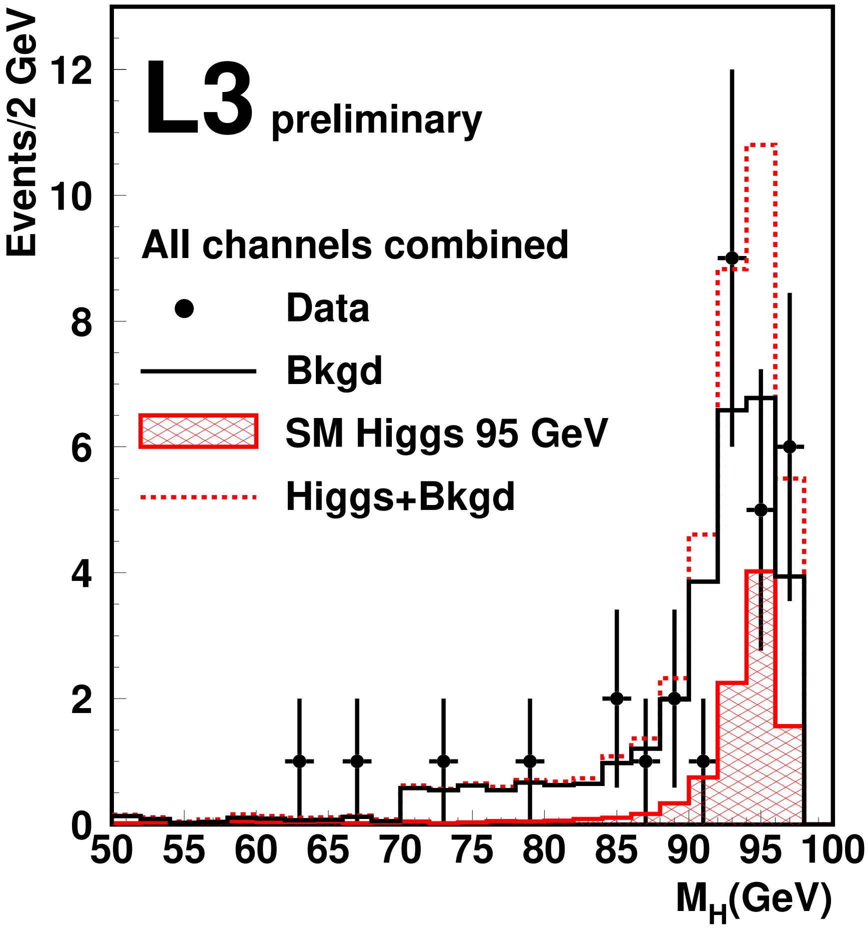

Figure 20: Mass distribution of Higgs candidates observed at $\sqrt{s} = 189$ GeV by the L3 experiment. The data are consistent with the background expectation consisting mainly of Z-pair production. The production of Higgs bosons, here shown for an hypothetical mass of 95 GeV, is not required.

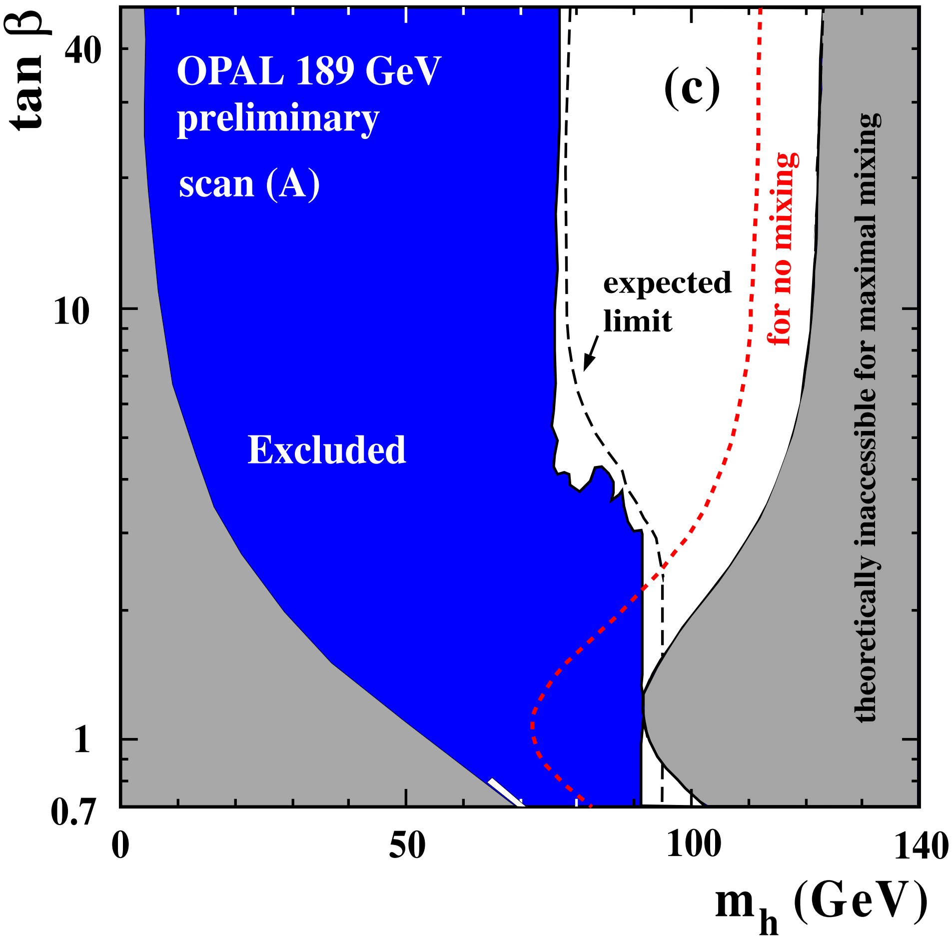

Figure 21: Lower mass limit on the h boson as a function of $\tan\beta$ obtained by the OPAL experiment.

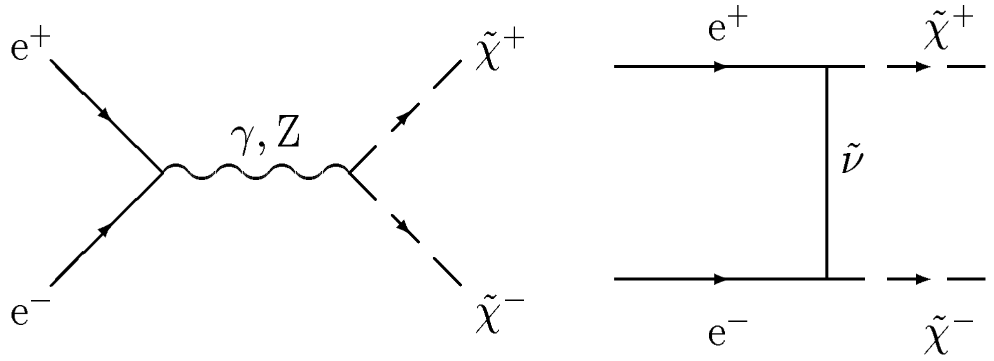

Figure 22: Feynman diagrams contributing to chargino pair production at LEP.

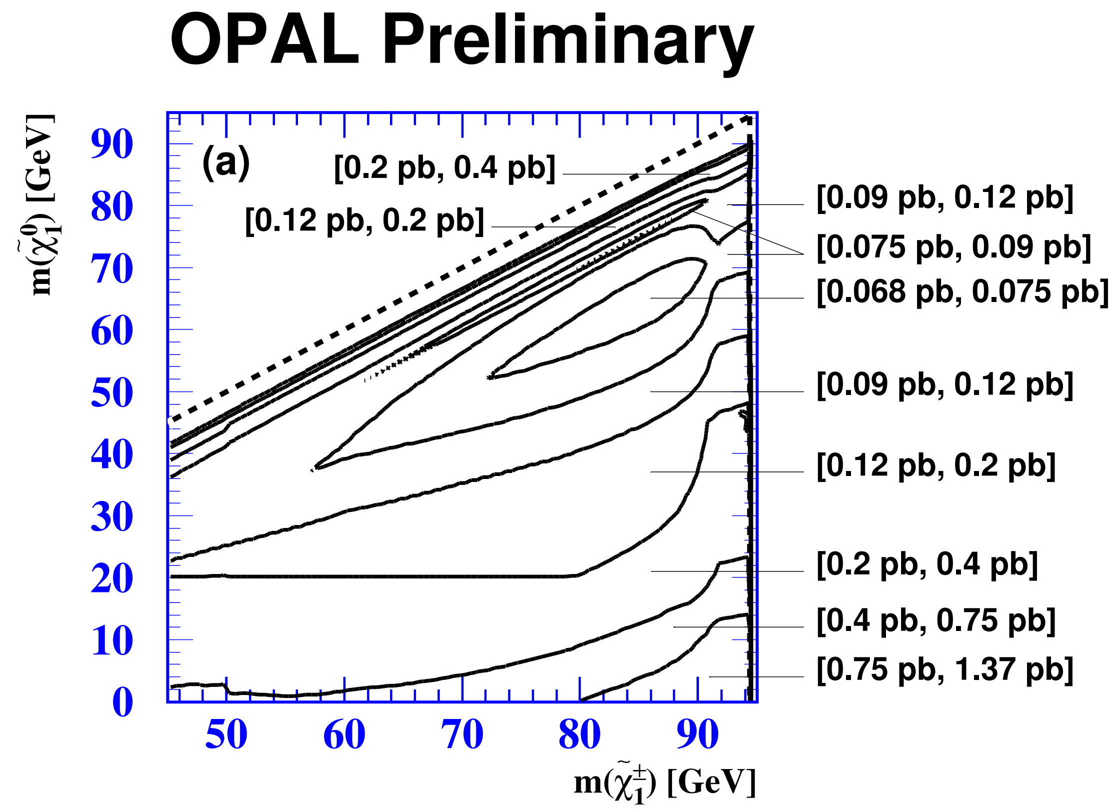

Figure 23: Upper experimental bounds on the cross section $e^+e^- \to \tilde{\chi}_1^+\tilde{\chi}_1^-$ at $\sqrt{s} = 189$ GeV obtained by the OPAL experiment as function of the chargino and neutralino masses.

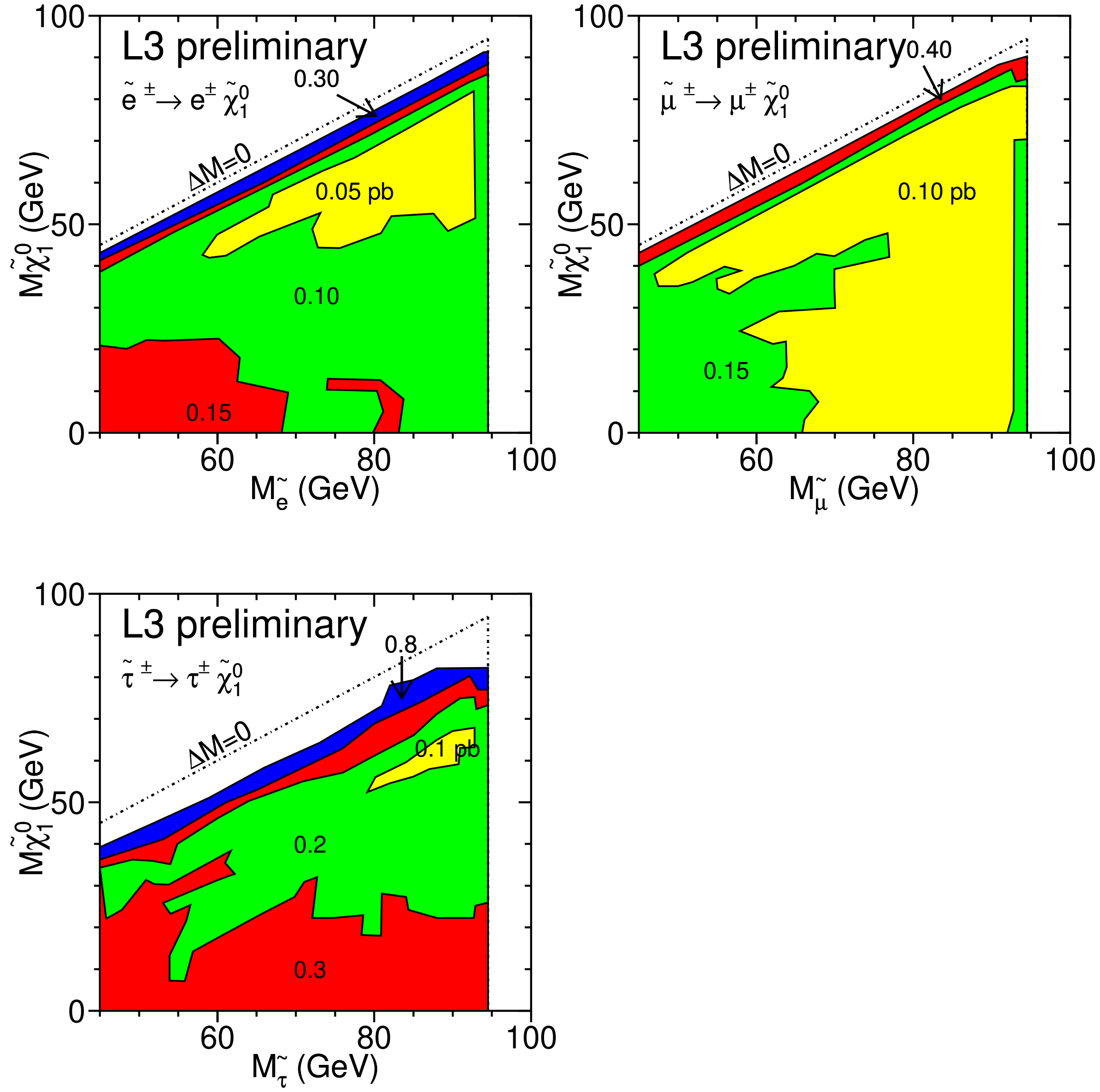

Figure 24: Upper experimental bounds on scalar lepton pair cross sections (in pb) at $\sqrt{s} = 189$ GeV obtained by the L3 experiment.

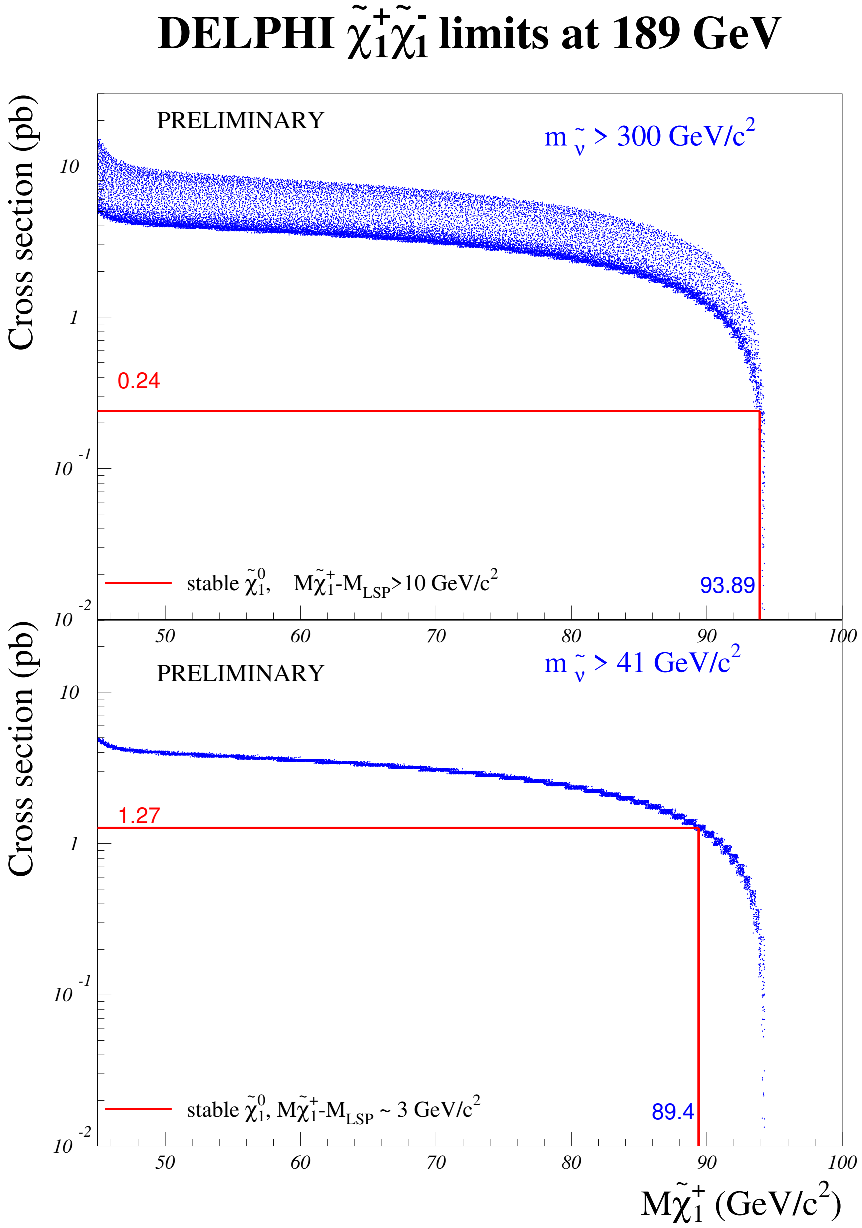

Figure 25: Expected MSSM cross section for chargino pair production at 189 GeV and preliminary chargino mass limits obtained by DELPHI.

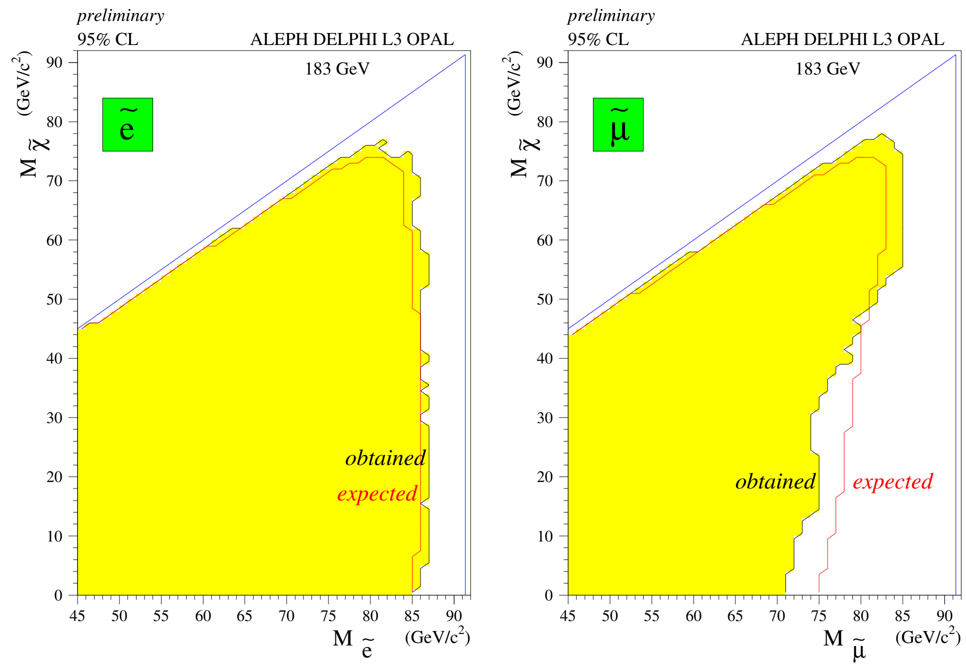

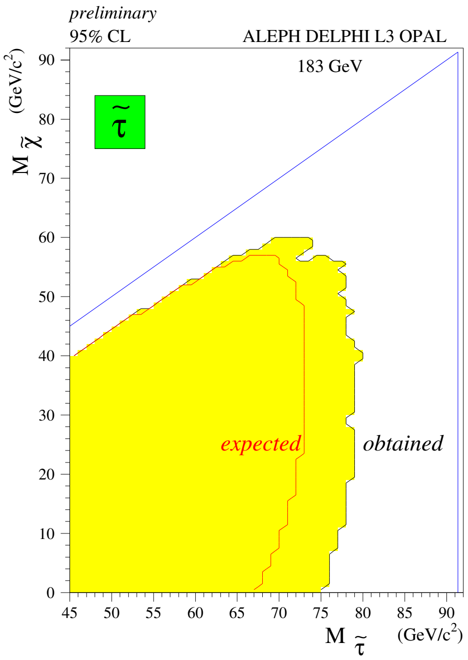

Combined LEP mass limits for $\Delta M > 20$ GeV

$$\begin{aligned} m_{\tilde{e}} &> 85 \text{ GeV} \\ m_{\tilde{\mu}} &> 71 \text{ GeV} \\ m_{\tilde{\tau}} &> 75 \text{ GeV} \end{aligned}$$

Figure 26: Exclusion in the $\tilde{\chi}_1^0 - \tilde{\ell}$ mass planes obtained from combining data of the four experiments up to $\sqrt{s} = 183$ GeV.

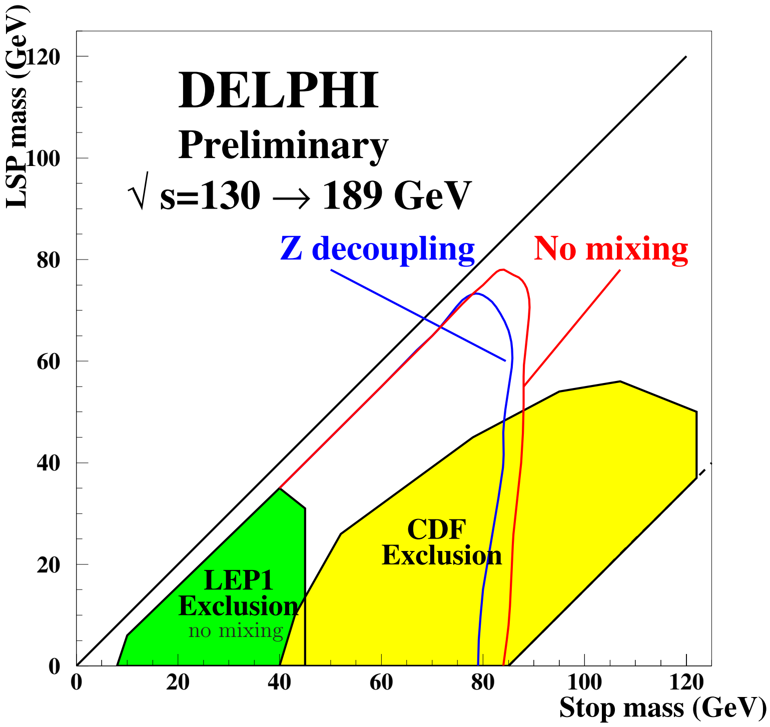

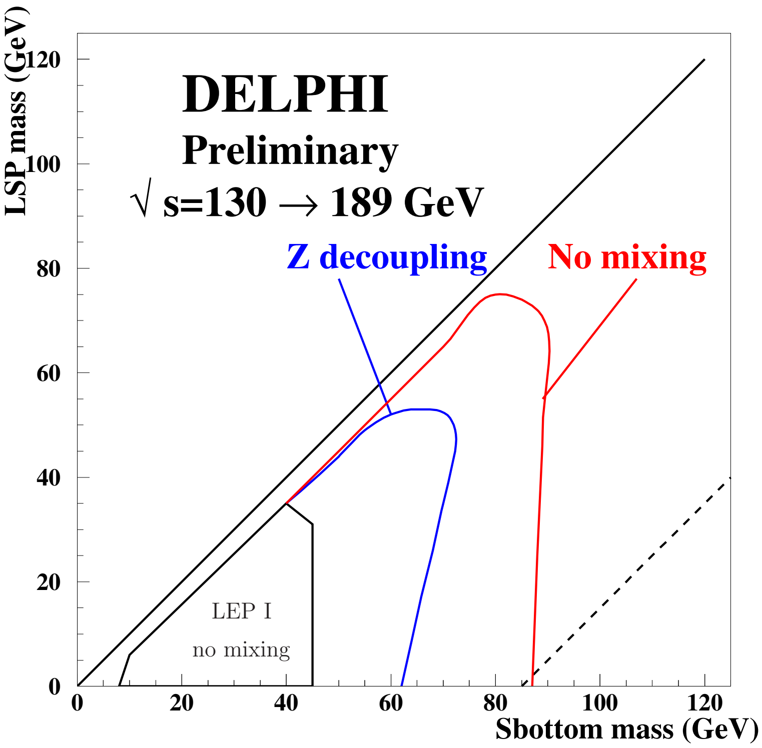

Figure 27: Exclusion region in the $\tilde{\chi}_1^0 - \tilde{t}_1$ and $\tilde{\chi}_1^0 - \tilde{b}_1$ planes. The results obtained by DELPHI at high cms energies are compared to the result derived from data at the Z resonance and, for the scalar top, to a search performed in $p\bar{p}$ collisions.

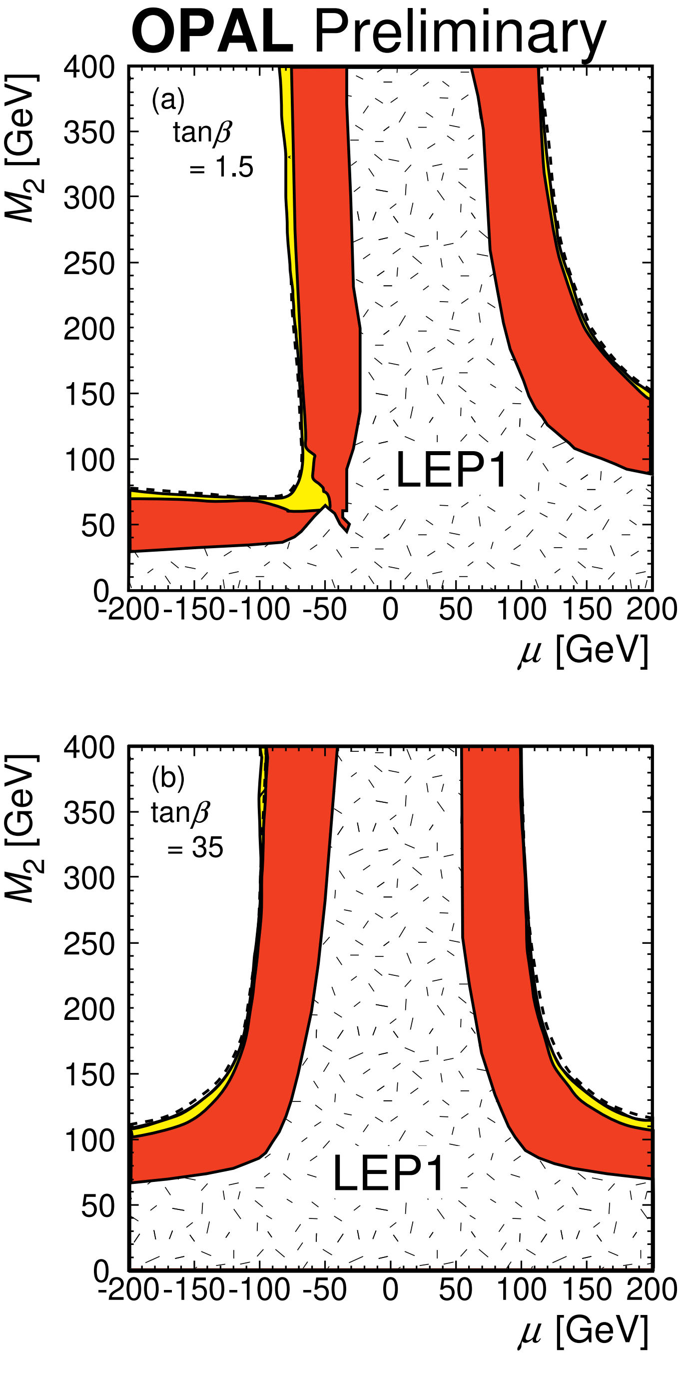

Figure 28: Exclusion region in the $\mu - M_2$ plane for two different values of $\tan\beta$. Regions already ruled out by LEP I data are shown with the additional exclusion obtained from data up to $\sqrt{s} = 189$ GeV. The dark shaded areas are excluded for all m_0 values and the light shaded areas are excluded additionally for $m_0 \geq 500$ GeV.

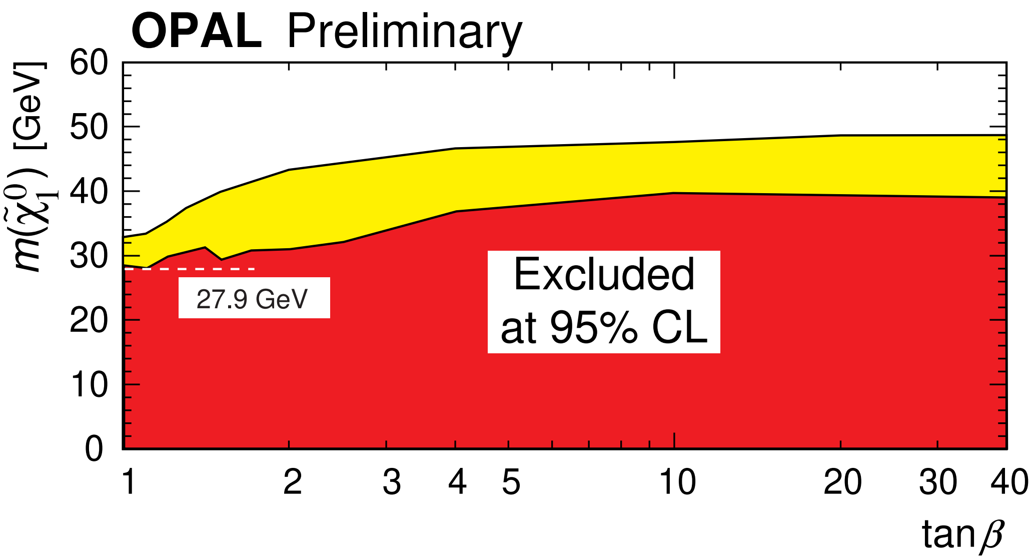

Figure 29: The lower mass limit on the lightest neutralino as function of $\tan\beta$. The dark shaded area is excluded for all choices of m_0 from which the absolute limit valid for all MSSM parameters is derived. The light shaded area is excluded with the assumption $m_0 \geq 500$ GeV.

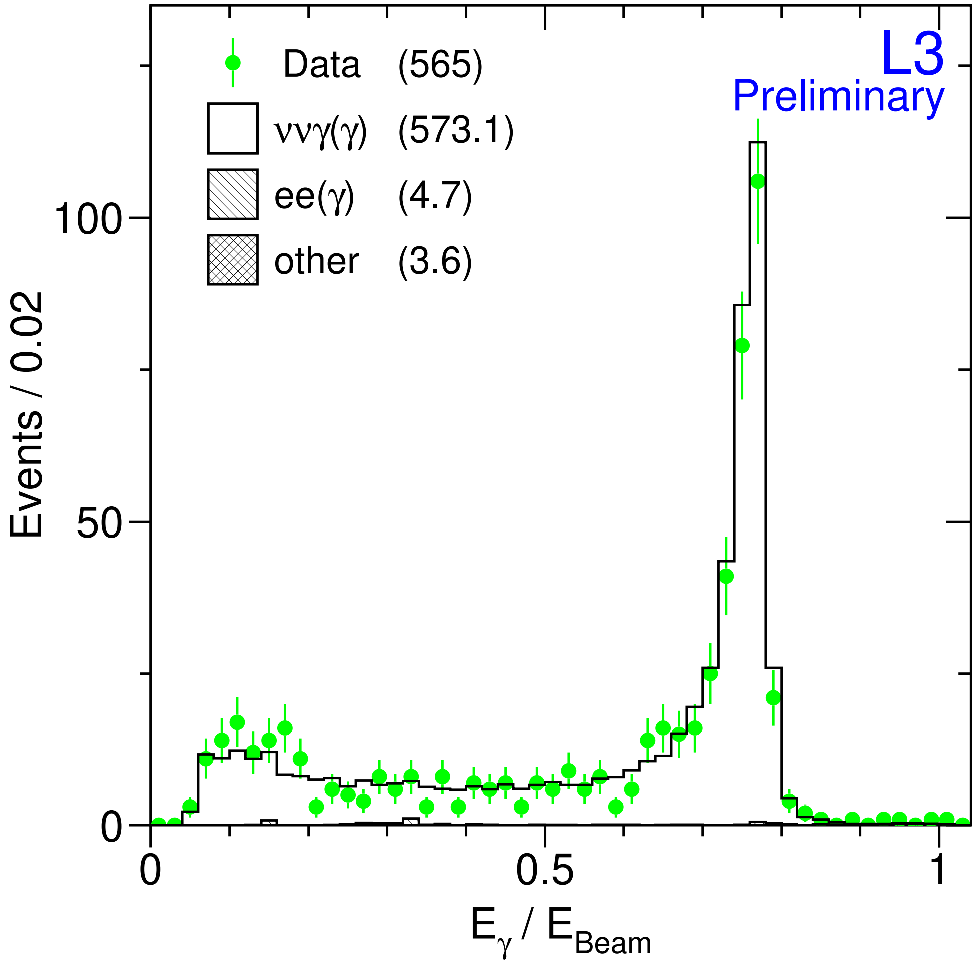

Figure 30: Spectrum of single photon events observed by L3 at $\sqrt{s} = 189$ GeV.

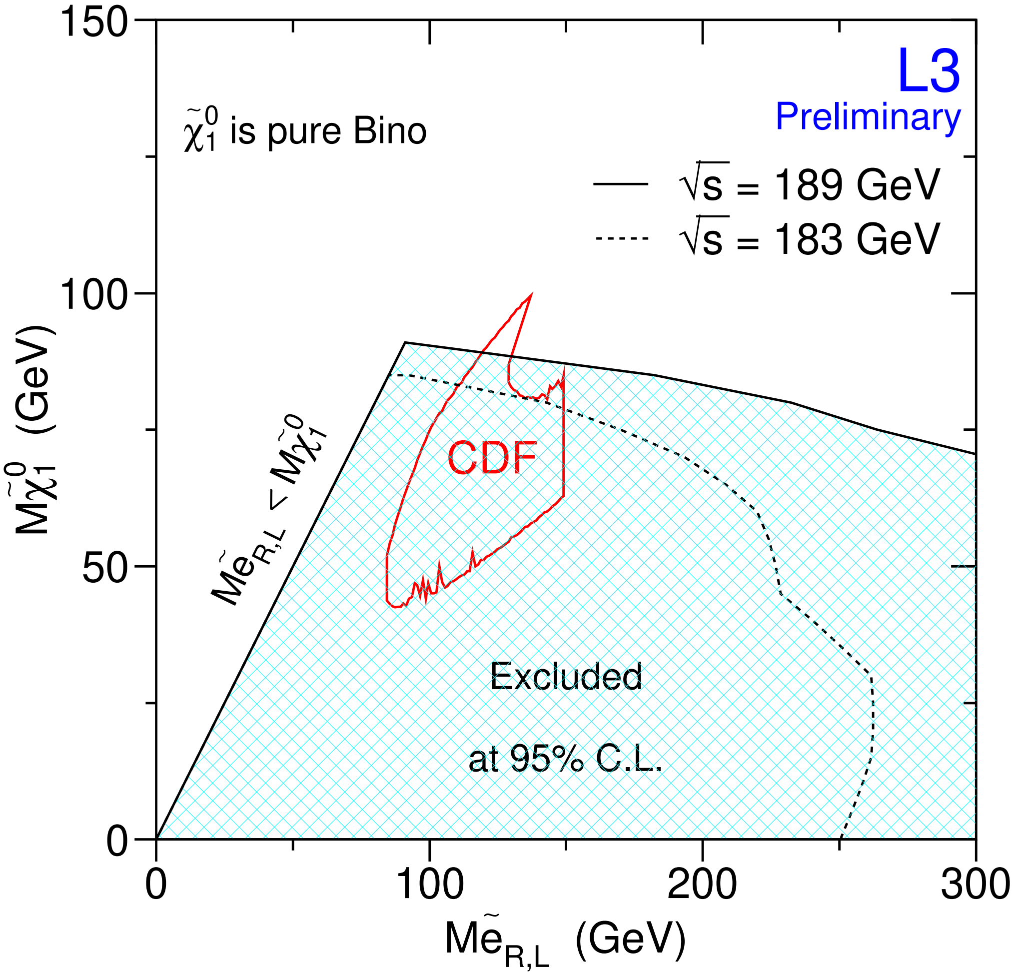

Figure 31: Excluded region in the $m_{\tilde{\chi}_1^0} - m_{\tilde{e}}$ plane from the study of di-photon events with missing energy. The kinematically allowed region of the CDF event when interpreted by the production of scalar electrons is shown for comparison.